The Astrophysical Journal, 755:163 (22pp), 2012 August 20 doi:10.1088/0004-637X/755/2/163

SIZING UP PARTIALLY DEPLETED GALAXY CORES

Bililign T. Dullo and Alister W. Graham
Centre for Astrophysics and Supercomputing, Swinburne University of Technology, Hawthorn, Victoria 3122, Australia; Bdullo@astro.swin.edu.au
Received 2012 February 20; accepted 2012 June 9; published 2012 August 7

ABSTRACT

We have modeled the inner surface brightness profiles of 39 alleged "core" galaxies with the core-Sérsic model, and provide new physical parameters for the largest ever sample of "core" galaxies fit with this model. When present, additional nuclear components were simultaneously modeled and the typical root-mean-square scatter of the fits (out to $\sim 10''$) is 0.02 mag arcsec^{-2}. Model-independent estimates of each core's break radius are shown to agree with those from the core-Sérsic model, and a comparison with the Nuker model is provided. We found an absence of cores in what amounts to 18% of the sample, which are reclassified here as Sérsic galaxies with low values of n ($\lesssim 4$) and thus shallow inner profile slopes. In general, galaxies with $n < 3$ and $\sigma < 183$ km s^{-1} do not have depleted cores. We derive updated relations between core-Sérsic break radii, their associated surface brightness, bulge luminosity, central velocity dispersion, and predicted black hole mass for galaxies with depleted cores. With the possible exception of NGC 584, we confirm that the inner negative logarithmic profile slopes γ are $\lesssim 0.3$ for the "core" galaxies, and $0 > \gamma > -0.1$ for six of these. Finally, the central stellar mass deficits are found to have values typically within a factor of four of the expected central black hole mass.

Key words: galaxies: elliptical and lenticular, cD – galaxies: fundamental parameters – galaxies: nuclei – galaxies: photometry – galaxies: structure

Online-only material: color figures

1. INTRODUCTION

The stellar distributions in galaxies have played a valuable role in guiding our understanding of the galaxies themselves. In particular, the accessibility of high-resolution imaging offered by the *Hubble Space Telescope* (*HST*) substantially advanced our appreciation of the complexity of galaxy cores (e.g., Crane et al. 1993; Kormendy et al. 1994; Jaffe et al. 1994; Ferrarese et al. 1994; Grillmair et al. 1994; van den Bosch et al. 1994; Lauer et al. 1995; Byun et al. 1996; Gebhardt et al. 1996; Carollo et al. 1997; Faber et al. 1997). For instance, the centers of real galaxies may contain such distinct components as bright active galactic nuclei (AGNs), nuclear star clusters, flattened nuclear disks and bars, dust lanes, and clouds. On the other hand, giant stellar evacuation zones are also observed. Luminous galaxies with such shallow cores had of course long been known to exist from ground-based observations (e.g., King & Minkowski 1966, 1972; King 1978; Young et al. 1978; Binney & Mamon 1982; see the review by Graham 2012a), but *HST* enabled us to accurately quantify these.

After studying 14 bright elliptical galaxies with the pre-refurbished *HST*/WFPC1, Ferrarese et al. (1994) introduced a four-parameter double power-law model to describe the inner surface brightness distributions of bright galaxies. While the (relatively brighter) galaxies in their sample, which possessed depleted cores with shallow inner profiles, were grouped as "Type I," the remaining galaxies, labeled "Type II," had a profile that remained steep all the way into the center. Examining a larger sample of galaxies imaged using the same *HST*/WFPC1 high-resolution Planetary Camera, Kormendy et al. (1994) and Lauer et al. (1995) largely agreed with the division of galaxies presented in Ferrarese et al. (1994), referring to them as "core" galaxies and "power-law" galaxies, respectively. They also advanced a double power-law model, which they dubbed the "Nuker law" for fitting the (underlying host galaxy) surface brightness profiles of early-type galaxies. The Nuker model has an additional fifth parameter to moderate the transition between the two power laws—as introduced by Hernquist (1990, his Equation (43)) for modeling the internal density profiles of galaxies.

The physical process(es) responsible for the observed difference between the inner surface brightness profiles of "core" galaxies and the fainter "power-law" galaxies (nowadays referred to as "Sérsic" galaxies because these spheroids have Sérsic light profiles rather than power-law light profiles) provide valuable clues about the galaxies' past history. In bright galaxies, the widely advocated "dry" (i.e., gas poor) galaxy merger hypothesis (e.g., Faber et al. 1997) can result in the gravitational sling shot of central stars (core scouring) due to the coalescence of supermassive black holes (SMBHs) from the progenitor galaxies (e.g., Begelman et al. 1980; Makino & Ebisuzaki 1996; Merritt & Milosavljević 2005; Merritt 2006). It is possible that the sizes and mass deficits of such partially depleted cores may reflect the amount of merging and damage caused by the black holes (after having eroded any pre-existing nuclear stellar components; Bekki & Graham 2010). Having an accurate quantification of the physical parameters defining the centers of galaxies is therefore important. Moreover, reliable break radii R_b, used to denote the sizes of the cores, may even be useful for predicting black hole masses (Lauer et al. 2007a).

While investigating the lack of any connection between the double power-law model and the curved galaxy brightness profiles observed outside of the cores, Graham et al. (2003, see their Figures 2–4) revealed that the Nuker model's break radius and other parameters were not robust quantities but are sensitive to the radial range of the surface brightness profile that is fitted. For example, the break radii R_b were shown to vary by more than a factor of three. The parameters' sensitivity was recognized to arise from the Nuker model's efforts to fit an outer power law to what is actually a curved brightness profile. The luminosity

profiles of bright (core) galaxies ($M_B \lesssim -20.5$ mag), which show a downward deviation from the inward extrapolation of their outer Sérsic (1963, 1968) profile, were subsequently shown to be precisely represented by the core-Sérsic model (Graham et al. 2003; Trujillo et al. 2004).

While Lauer et al. (2005) missed this development, Ferrarese et al. (2006) found the core-Sérsic model to be highly applicable to bright early-type galaxies in the Virgo cluster. Lauer et al. (2007a, 2007b) subsequently wrote that "Graham et al. (2003) have criticized the Nuker r_b as being sensitive to the domain over which the Nuker law was fitted, particularly when the outer limit of the fit extends only slightly beyond r_b. In practice, however, the Nuker laws are fitted over a large radial range that extends well beyond r_b." However, this was not the problem identified by Graham et al. (2003), who had demonstrated that the Nuker model parameters deviated further from the true values as the fitted radial extent was *increased*.

Based on work "in preparation," Lauer et al. (2007b, p. 242) refuted that their Nuker break radii were biased "in any way" because their radii reportedly agreed very well with model-independent values of where the curvature in the surface brightness profile was a maximum. This was a surprising claim because these latter values should not be dependent on the radial extent of the data while the Nuker model break radii *are* a strong function of the fitted radial extent (Graham et al. 2003). Kormendy et al. (2009, their Section 4.1) subsequently buoyed the Nuker model and dismissed the core-Sérsic model. Gültekin et al. (2009) then overlooked any and all concerns about the Nuker model, which they presented along with Nuker model parameters from Lauer et al. (2005), and encouraged readers to use these data, additionally noting that the surface brightness profiles that were fit with the Nuker model are available at the Nuker Web site.[1] Gültekin et al. (2011) continued in this vein, motivating us to further investigate, nearly a decade on, the issue of whether the Nuker model parameters are reliable, physically meaningful quantities, or if instead the core-Sérsic model parameters may be preferable. At stake is not only the accuracy to which we quantify the cores of galaxies, but our subsequent understanding of cores and how they relate to their galaxy at large.

In this paper, we focus on the nuclear structure of galaxies by re-analyzing the surface brightness profiles of all 39 "core" galaxies imaged with the WFC2/*F*555*W* or *F*606*W* filter and listed in Lauer et al. (2005) to be a "core" galaxy (see Section 2). For reference, Trujillo et al. (2004) modeled only nine possible "core" galaxies, Ferrarese et al. (2006) modeled 10, and Richings et al. (2011) have very recently modeled 21 "core" galaxies. We are therefore modeling the largest sample of suspected "core" galaxies to date. For comparison's sake with the Nuker model break radii, we use exactly the same surface brightness profiles as Lauer et al. (2005), available at the previously mentioned Nuker Web site.

We first concentrate on measuring the core size using the core-Sérsic model (see Sections 3 and 4). We additionally take the nuclear excess, usually nuclear star clusters or AGN emission, into account while modeling the underlying host galaxy light. In Section 5, we use two model-independent core size estimators and reveal that one of these cannot be used while the other is consistent with our core-Sérsic break radii. Furthermore, we confirm that the published Nuker model break radii are typically 100% larger than the break in the surface brightness profile determined relative to the inward extrapolation of the outer Sérsic function (Trujillo et al. 2004). We additionally report that "artificial" break radii have been reported in what were alleged to be "core" galaxies but are actually Sérsic galaxies with no break in their Sérsic profile and which thus have no partially depleted core relative to their outer light profile (Section 6). Throughout this paper, we use terms such as "actual," "true," and "real" break radii and cores when referring to galaxies that have inner surface brightness profiles that break downward from (i.e., have lower flux than) the inward extrapolation of the outer Sérsic model, which describes their outer stellar distribution.

Sets of structural parameter relations encompassing central as well as global properties are presented in Section 7. In particular, equations involving the break radius and associated surface brightness, and the luminosity, are derived. We also investigate the core size–central black hole mass relation in Section 7.2. Using updated data, we find that the break radius *can* be used to consistently predict the black hole mass when using either the $M_{\rm bh}$–σ or $M_{\rm bh}$–L relations for "core" galaxies when coupled with our updated R_b–σ and R_b–L relations. We go on to discuss the detection of additional nuclear components in the full sample of Sérsic and core-Sérsic galaxies in Section 8 while Section 9 summarizes our main conclusions.

2. SAMPLE SELECTION

Lauer et al. (2005) analyzed and presented fits to the major-axis surface brightness profiles of 77 relatively bright, nearby, early-type galaxies. Every galaxy in their sample was observed with the Wide Field Planetary Camera 2 (WFPC2: Biretta et al. 2001) onboard the *HST* and was centered on the PC CCD (which has an image scale of $0\farcs0456$ pixel^{-1} and a field view of 800 × 800 pixels). Their sample lacks any characterizing selection criteria and comprises galaxies at distances of ∼10–100 Mpc. While almost all of the "core" galaxies were imaged with the *F*555*W* filter (similar to broadband *V*), two were not and we use their *F*606*W* data (roughly broadband *R*) instead. We refer the reader to Lauer et al. (2005) for an extensive description of the sample and images, which includes procedures adopted for point spread function (PSF) deconvolution,[2] dust obscuration correction, sky subtraction, and background source masking.

Our sample comprises 39 early-type galaxies, which are the "core" galaxy subset of the 77 galaxies presented in Lauer et al. (2005). This sample selection enables a direct comparison with the (published) Nuker model's estimation of the core size and related parameters, and to further achieve this direct comparison we have modeled the same published light profiles.[1] The global properties of our target galaxies are summarized in Table 1, which presents their morphology, magnitude, updated distance, and velocity dispersion. For the six lenticular galaxies plus one Sa spiral galaxy, we have roughly converted their total galaxy magnitudes, reported by Lauer et al. (2007b), into bulge magnitudes using a mean *V*-band bulge-to-disk ratio of 1/3, equivalent to a mean bulge-to-total ratio of 1/4 (Graham & Worley 2008; Laurikainen et al. 2010, their Section 6.3, and references therein). The 1σ range on this B/T ratio for S0–Sa galaxies is about a factor of two, corresponding to a 1σ uncertainty of ±0.75 mag for our bulge magnitudes. In passing, we note that for four of these seven disk galaxies (NGC 507,

[1] http://www.noao.edu/noao/staff/lauer/wfpc2_profs/

[2] Some of the merits and disadvantages of image deconvolution are described in Ferrarese et al. (2006).

Table 1
Updated Global Parameters of the "Core" Galaxy Sample from Lauer et al. (2005)

Galaxy	Type	M_V (mag)	D (Mpc)	σ (km s^{-1})
(1)	(2)	(3)	(4)	(5)
NGC 0507	S0	−21.54	63.7^n	306
NGC 0584	E	−21.12	19.6^t	206
NGC 0741	E	−23.31	72.3^n	291
NGC 1016	E	−23.22	88.1^n	302
NGC 1374	E	−20.39	19.2^t	183
NGC 1399	E	−21.89	19.4^t	342
NGC 1700	E	−22.53	53.0^n	239
NGC 2300	S0	−19.90	25.7^n	261
NGC 3379	E	−20.86	10.3^t	209
NGC 3607	S0	−19.95	22.2^t	224
NGC 3608	E	−21.05	22.3^t	192
NGC 3640	E	−21.80	26.3^t	182
NGC 3706	S0	−20.56	45.2^n	270
NGC 3842	E	−23.04	91.0^n	314
NGC 4073	cD	−23.33	85.3^n	275
NGC 4278	E	−20.90	15.6^t	237
NGC 4291	E	−20.68	25.5^t	285
NGC 4365	E	−22.00	19.9^t	256
NGC 4382	S0	−20.47	17.9^t	179
NGC 4406	E	−22.31	16.7^t	235
NGC 4458	E	−19.13	16.8^t	103
NGC 4472	E	−22.66	15.8^t	294
NGC 4473	E	−20.82	15.3^t	179
NGC 4478	E	−19.85	17.6^t	137
NGC 4486B	cE	−18.77	25.8^n	170
NGC 4552	E	−21.25	14.9^t	253
NGC 4589	E	−21.01	21.4^t	224
NGC 4649	E	−22.32	16.4^t	335
NGC 5061	E	−22.43	32.6^n	186
NGC 5419	E	−23.27	59.9^n	351
NGC 5557	E	−22.34	46.4^n	253
NGC 5576	E	−21.11	24.8^t	171
NGC 5813	E	−22.20	31.3^t	237
NGC 5982	E	−22.04	41.8^n	239
NGC 6849	SB0	−21.21	80.5^n	209
NGC 6876	E	−23.45	54.3^n	229
NGC 7213	Sa	−20.38	21.1^n	163
NGC 7619	E	−22.76	51.5^t	323
NGC 7785	E	−21.96	47.2^n	255
NGC 0596*	cD	−20.81	21.2^t	151
NGC 1426*	E	−20.51	23.4^t	151

Notes. Column 1: galaxy name. Column 2: morphological classification from the NASA/IPAC Extragalactic Database (NED; http://nedwww.ipac.caltech.edu). Column 3: absolute V-band (galaxy or bulge) magnitude obtained from Lauer et al. (2007b) and adjusted using the distance from Column 4. Sources: (t) Tonry et al. (2001) after reducing their distance moduli by 0.06 mag (Blakeslee et al. 2002); (n) from NED (3K CMB). Column 5: central velocity dispersion from HyperLeda (http://leda.univ-lyon1.fr; Paturel et al. 2003). The superscript "*" is used to indicate two "power-law" galaxies taken from Lauer et al. (2005) and used for illustrative purpose in Figure 1.

NGC 2300, NGC 3607, and the Sa galaxy NGC 7213), the dust-corrected K-band B/T ratios reported by Laurikainen et al. (2010) are 0.33, 0.28, 0.33, and 0.18, respectively, suggesting that we are not too far off with our adopted B-band value of 0.25. Laurikainen et al. do however identify NGC 3706 as an elliptical galaxy, while de Vaucouleurs et al. (1991) refer to it as SA0(rs), and we have no comparison B/T ratios for NGC 4382 and NGC 6849. In any event, it should be remembered that these latter three galaxies make up a fairly small fraction of the total sample.

3. THE SÉRSIC AND CORE-SÉRSIC MODELS

By combining CCD images of early-type Virgo cluster galaxies with deep, large field-of-view, photographic images, Caon et al. (1993) revealed that the Sérsic (1963) model fits the main parts of the profiles of both elliptical and spheroidal galaxies astonishingly well over large ranges in surface brightness (down to ∼29 B-mag arcsec^{-2}). In general, after excluding the nuclear region, the Sérsic $R^{1/n}$ model fits the surface brightness profile of both elliptical galaxies and the bulges of disk galaxies remarkably well over their entire radial range (Caon et al. 1993; D'Onofrio et al. 1994; Young & Currie 1994; Andredakis et al. 1995; Graham et al. 1996). In fact, systematic deviations from this model appear to signal either the presence of a central light deficit or an additional nuclear component (Balcells et al. 2003; Graham & Guzmán 2003). Indeed, using CCD images with the extended profiles from Caon et al. (1993) and other photographic data, one of main conclusions noted in Kormendy et al. (2009) was exactly this.

The radial intensity distribution of the three-parameter Sérsic $R^{1/n}$ model, a generalization of de Vaucouleurs (1948) two-parameter $R^{1/4}$ model, is defined as

$$I(R) = I_e \exp\left\{-b_n\left[\left(\frac{R}{R_e}\right)^{1/n} - 1\right]\right\}, \quad (1)$$

where I_e denotes the intensity at the half-light radius R_e. The quantity $b_n \approx 2n - 1/3$, for $1 \lesssim n \lesssim 10$ (e.g., Caon et al. 1993), is a function of the shape parameter n, and is defined in a way to ensure that R_e encloses half of the total luminosity. A review of the Sérsic model and its associated expressions can be found in Graham & Driver (2005).

Many, but not all, spheroids fainter than −20.5 B-mag contain additional nuclear components. This is illustrated in Figure 1 where we display a Nuker model and a Sérsic plus point-source model fit to the surface brightness profiles of NGC 596 and NGC 1426. The profiles have been taken from the Nuker Web sites, and the fitted Nuker model parameters are from Lauer et al. (2005). Both models agree on the absence of a partially depleted core, and as such the galaxies are classified as Sérsic galaxies. There are, however, considerable differences regarding the quality of the fits. For NGC 596, the three-parameter Sérsic plus two-parameter Gaussian model accommodates the entire observed radial range of the brightness profile remarkably well with a smaller root-mean-square (rms) residual than the five-parameter Nuker model. The Nuker model fit (taken from Lauer et al. 2005) to this galaxy's light profile not only excluded the inner most data points but also clearly reveals a significant departure from the profile in the outer region. Similarly, while the Sérsic model plus Gaussian function can represent the entire observed profile of NGC 1426, the five-parameter Nuker model cannot describe the extra compact light source at the center and has more scatter in the residual profile.

As mentioned previously, the light profiles of luminous ($M_B \lesssim -20.5$ mag) elliptical galaxies depart systematically from the Sérsic model near their center. It is important to realize that this departure, a downward deviation with respect to the inward extrapolation of the outer Sérsic profile, emanates from a central starlight deficit and is not due to dust (which would result in a dramatic color change). Such stellar distributions can be described using the core-Sérsic model introduced by Graham et al. (2003) and applied in Trujillo et al. (2004). A blend of an inner power law and an outer Sérsic function, the core-Sérsic

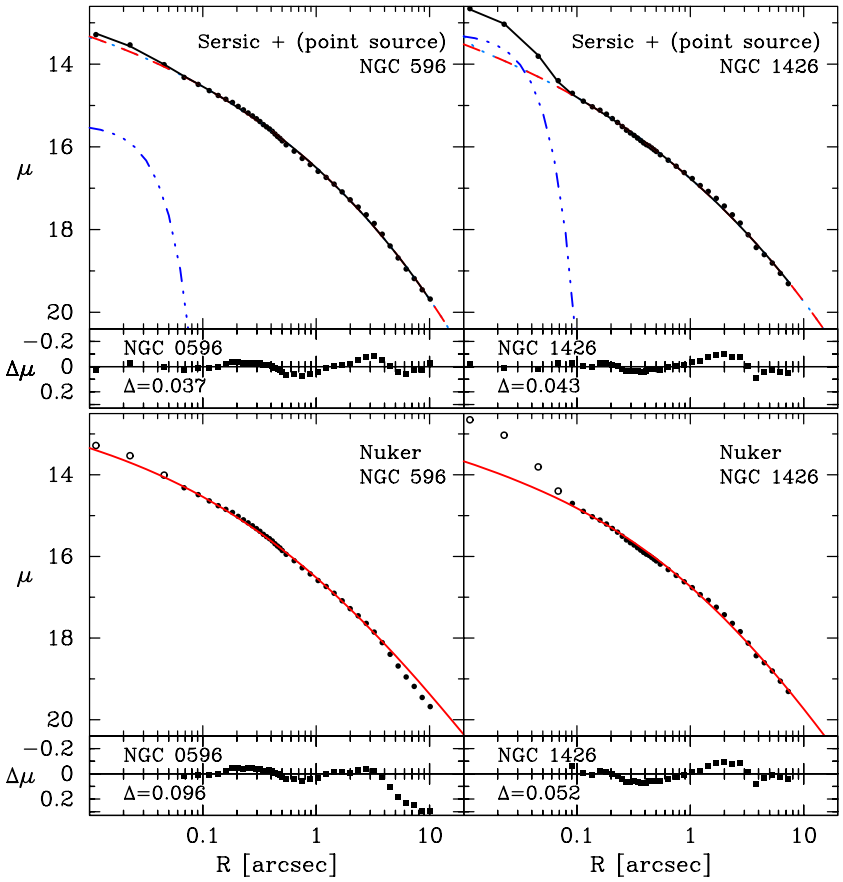

Figure 1. Left panel: a three-parameter Sérsic plus two-parameter point-source model describes the entire available radial extent of NGC 596 while the five-parameter Nuker model (fit taken from Lauer et al. 2005) fails to describe the inner and outer light profiles. Right panel: a three-parameter Sérsic plus two-parameter point-source model describes NGC 1426 better than the five-parameter Nuker fit taken from Lauer et al. (2005) which cannot describe the nucleus. The rms scatter, Δ, about the major axis, *F*555*W*-band surface brightness profiles pertains only to the data points included in the fit (shown by the filled symbols).

(A color version of this figure is available in the online journal.)

model can be written as

$$I(R) = I' \left[1 + \left(\frac{R_b}{R}\right)^{\alpha}\right]^{\gamma/\alpha} \exp\left[-b\left(\frac{R^{\alpha} + R_b^{\alpha}}{R_e^{\alpha}}\right)^{1/(\alpha n)}\right], \quad (2)$$

with

$$I' = I_b 2^{-\gamma/\alpha} \exp[b(2^{1/\alpha} R_b/R_e)^{1/n}], \quad (3)$$

where I_b is intensity at the core's break radius R_b, γ is the slope of the inner power-law region, and α controls the sharpness of the transition between the inner power-law and the outer Sérsic profile. As in the Sérsic model, R_e is the effective half-light radius of the outer Sérsic function and b has the same general definition as before.[3] In practice, the six-parameter core-Sérsic model can be reduced to a five-parameter model by setting α to some large constant value. Trujillo et al. (2004) set $\alpha \to \infty$, so that the transition from Sérsic profile to power law at R_b is infinitely sharp, with no transition region, an approach effectively adopted by Ferrarese et al. (2006). In this paper, as in Richings et al. (2011), we explore and use a range of finite values for α.

4. FITTING ANALYSIS

We fit the one-dimensional light distributions of the 39 underlying host galaxies using Sérsic and core-Sérsic models, and account for any additional nuclear light components with either a Gaussian or an exponential model. Fits to the full 39 galaxies are available in Appendix A. The quality of the fits, as indicated by the rms given in each panel of Figure 21, is excellent, typically 0.01–0.03 mag arcsec^{-2}.

As can be seen, the three-parameter Sérsic model proffers a good match to two (NGC 4473 and NGC 5576) of the 39 galaxies[4] all the way to the *HST* resolution limit. While these galaxies have shallow central profiles, the profiles do not "break" from the outer envelope—further evidenced by the small values of α used with the Nuker model (Lauer et al. 2005). Application of the Sérsic model, along with small inner Gaussian and exponential functions, yields a satisfactory fit to the luminosity profiles of an additional five nucleated galaxies (NGC 1374, NGC 4458, NGC 4478, NGC 4486B, and NGC 7213). In what follows, and as noted before, we collectively refer to this class of galaxy without depleted cores as "Sérsic" galaxies, as done by Trujillo et al. (2004), who first reported that NGC 4458 and NGC 4478 are Sérsic galaxies, i.e., they do not display any *downward* departure from the Sérsic $R^{1/n}$ profile at their centers. Kormendy et al. (2009) and Hopkins et al. (2009) also

[3] One recovers the Sérsic $R^{1/n}$ function from Equation (2) when setting R_b and γ to zero.

[4] The Nuker model parameterization (Lauer et al. 2005) reported that NGC 4473 and NGC 5576 had break radii of 4.45 and 4.18 arcsec, respectively.

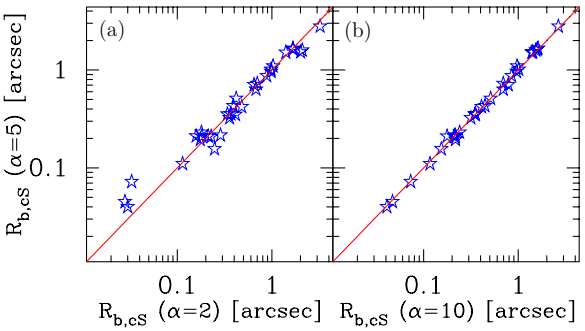

Figure 2. Robustness of the core-Sérsic break radii. Break radii from moderate-transition, $\alpha = 5$, core-Sérsic fits plotted against (a) break radii from broad-transition fits, $\alpha = 2$ and (b) sharp-transition fits, $\alpha = 10$. The Pearson correlation coefficient (r) between $R_{b,cS}$ ($\alpha = 5$) and $R_{b,cS}$ ($\alpha = 2$) is 0.99, while r of $R_{b,cS}$ ($\alpha = 5$) vs. $R_{b,cS}$ ($\alpha = 10$) is 1.0.

(A color version of this figure is available in the online journal.)

identify central light excesses over the Sérsic function in these two galaxies. Except for NGC 4486B (Lauer et al. 1996) and NGC 7213, the rms residual scatter is $\lesssim$0.032 mag arcsec^{-2} for these seven Sérsic galaxies. These two exceptions are two of only four galaxies, from the full sample of 39, with complicated structure (see Appendix A, Figure 23). As shown in Section 6, these seven galaxies stand out from the "core" galaxies in a number of systematic ways.

There is some variation in α from galaxy to galaxy when using the core-Sérsic model. The role of the parameter α is to moderate the sharpness of the transition between the outer Sérsic profile and the inner power law, with higher values corresponding to sharper transitions and vice versa. The profile of NGC 4291, for example, has a sharper transition and hence requires a larger value of α than say NGC 1399. We have set $\alpha = 10, 5$, and 2 for matching sharp, moderate, and broad transition regions, respectively. The change in the core size, i.e., the break radius, while varying α has been closely inspected. The robustness of the break radius is illustrated by the plots shown in Figure 2, which compare the break radii obtained using different values of α. The Pearson correlation coefficient (r) between the core-Sérsic break radius $R_{b,cS}(\alpha = 10)$ and the core-Sérsic break radius $R_{b,cS}(\alpha = 5)$ shown in Figure 2(b) is 1.0. Although the break radii from the broad-transition model (i.e., using $\alpha = 2$) has a small amount of scatter in Figure 2(a), this is due to the fact that the majority of our sample galaxies do not prefer the broad-transition model. There are, however, a small handful of galaxies (NGC 1016, NGC 1399, NGC 2300, NGC 3379, NGC 4365, NGC 4649, NGC 5419, and NGC 5813) whose profiles have a broad transition region (see Table 2).

We also estimate the uncertainties of the core-Sérsic model parameters by exploring their stability for different α values (i.e., 2, 5, and 10). In agreement with Richings et al. (2011) and Trujillo et al. (2004), for some galaxies, we notice that γ, n, and R_e obtained from the best $\alpha = 5$ and 10 fits are slightly different from the ones which are obtained using $\alpha = 2$.

In addition, we explore the coupling between the core-Sérsic break radius R_b and the Sérsic index n by holding the other parameters constant at their best-fit values (Table 2) and using the χ^2 distribution, which we normalized at the minimum value. In Figure 3, we show the 68.3% (1σ) confidence limits around the optimal R_b and n values for the core galaxies using the $\Delta\chi^2 = 1.0$ contours after marginalizing over the remaining core-Sérsic parameters. In general, Figure 3 indicates the absence of a coupling between R_b and n, as seen by the small

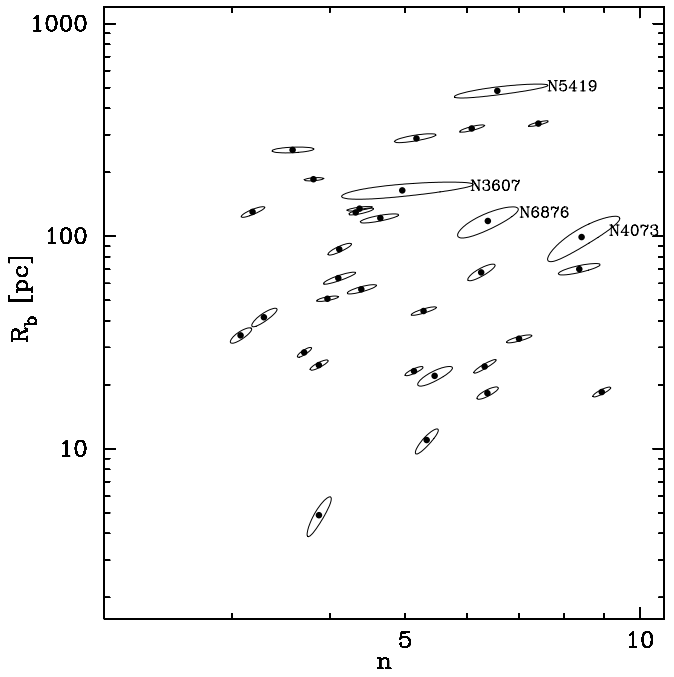

Figure 3. Parameter coupling between the core-Sérsic break radius R_b and Sérsic index n for our "core" galaxy sample. The contours show the $\Delta\chi^2 = 1$ boundaries, and their projections onto the horizontal and vertical axes give the 68.3% (1σ) confidence intervals around each galaxies' optimal n and R_b values, respectively. Each contour is generated by holding all the core-Sérsic parameters, other than R_b and n, fixed at their best-fit values (Table 2).

contours. Overall, we estimate the uncertainties associated with γ, R_b, n, and R_e to be roughly 10%, 10%, 15%, and 20%, respectively. We also note that the errors in the Sérsic parameters could partly be associated with the limited radial extent of our data (see Section 4.1).

As noted in passing above, only four galaxies are somewhat poorly represented using our models (NGC 4073, NGC 4486B, NGC 6876, and NGC 7213; see Appendix A, Figure 23). NGC 7213 is a Seyfert (Sa) galaxy with a winding nuclear dust spiral, which can be traced all the way to the nucleus (Deo et al. 2006). It appears that this prominent dusty nuclear feature in the galaxy profile (see Figure 4), which the core-Sérsic model is not designed to recover, is the likely origin for the residual pattern about the model fit to this galaxy, particularly in the inner $R \lesssim 0\farcs3$ region. The cD galaxy, NGC 4073, has an inner ring (Lauer et al. 2005) over the $0\farcs1 < R < 0\farcs4$ region and we exclude these few data points from the fit. NGC 6876 is a dominant elliptical galaxy in the Pavo group with a possible past or ongoing merger history (Machacek et al. 2005). The residual structures outside the core regions of NGC 4073 and NGC 6876 that are seen in Figure 23 seem to be associated with the change in ellipticities of these galaxies as presented by Lauer et al. (2005). Finally, although not apparent from the I and V broadband *HST*/WFPC2 image, Lauer et al. (1996) remarked on the presence of a double optical nucleus from the deconvolved WFPC2 image of NGC 4486B. This creates a spurious depleted core as noted by Lauer et al. (1996); see also Soria et al. (2006) and Ferrarese et al. (2006).

4.1. Literature Comparison of Core-Sérsic Fits

We have seven galaxies (NGC 1700, 4291, 4458, 4478, 5557, 5576, and 5982) in common with Trujillo et al. (2004) and 10 galaxies (NGC 4365, 4382, 4406, 4458, 4472, 4473, 4478,

Table 2
Structural Parameters

Galaxy	$\mu_{b,V}$ (mag arcsec^{-2})	R_b (arcsec)	R_b (pc)	γ	α	n	Profile Type	$m_{\rm pt,V}$ (mag)	$\mu_{0,V}$ (mag arcsec^{-2})	h (arcsec)	Notes
(1)	(2)	(3)	(4)	(5)	(6)	(7)	(8)	(9)	(10)	(11)	(12)
NGC 0507	16.45	0.42	130	0.09	5	3.2	*c-S*				
NGC 0584	14.57	0.19	18	0.46	5	6.4	*c-S*				
NGC 0741	17.52	0.96	338	0.19	5	7.4	*c-S*	22.4			
NGC 1016	17.21	0.68	289	0.20	2	5.2	*c-S*				
NGC 1374^{+}	–	–	–	–	–	2.8	*S*		14.3	0.17	
NGC 1399^{+}	16.29	2.09	196	0.11	2	4.0	*c-S*				
NGC 1700	13.64	0.07	18	0.27	5	8.9	*c-S*				
NGC 2300	16.85	0.98	122	0.11	2	4.7	*c-S*				
NGC 3379	15.66	1.03	51	0.19	2	4.0	*c-S*				
NGC 3607	16.42	1.52	164	0.29	5	5.0	*c-S*				Nuclear dust lanes
NGC 3608	15.10	0.21	23	0.28	5	5.1	*c-S*				
NGC 3640	14.72	0.04	5	−0.02	5	3.9	*c-S*				
NGC 3706	14.17	0.11	24	−0.02	10	6.3	*c-S*				Ring of stars (0.″06–0.″4)
NGC 3842	17.42	0.72	320	0.19	5	6.1	*c-S*				
NGC 4073	16.47	0.24	99	−0.05	10	8.4	*c-S*				Ring of stars (0.″1–0.″4)
NGC 4278	15.79	0.75	56	0.20	5	4.4	*c-S*	19.4			
NGC 4291	15.22	0.35	44	0.10	5	5.3	*c-S*				
NGC 4365	16.56	1.40	135	0.04	2	4.4	*c-S*	20.1			
NGC 4382	15.04	0.32	28	0.08	5	3.7	*c-S*				
NGC 4406	16.01	0.87	70	0.01	5	8.4	*c-S*				
NGC 4458	–	–	–	–	–	3.1	*S*	17.0	14.4	0.25	
NGC 4472	16.44	1.68	129	0.00	2	4.3	*c-S*	22.2			
NGC 4473	–	–	–	–	–	2.1	*S*				
NGC 4478	–	–	–	–	–	2.7	*S*	20.1	15.6	0.41	
NGC 4486B	–	–	–	–	–	3.0	*S*				Double optical nuclei
NGC 4552	15.00	0.35	25	0.01	10	3.9	*c-S*	20.5			
NGC 4589	15.34	0.21	22	0.30	5	5.5	*c-S*				
NGC 4649	16.92	3.23	256	0.18	2	3.6	*c-S*				
NGC 5061	14.06	0.21	33	0.13	5	7.0	*c-S*				
NGC 5419	17.60	1.67	485	−0.05	2	6.6	*c-S*	19.9			
NGC 5557	15.31	0.16	35	0.17	5	3.1	*c-S*				
NGC 5576	–	–	–	–	–	3.5	*S*				
NGC 5813	16.15	0.42	64	−0.09	2	4.1	*c-S*				
NGC 5982	15.45	0.21	42	0.08	5	3.3	*c-S*				
NGC 6849	16.72	0.22	84	0.20	5	6.3	*c-S*				
NGC 6876	16.98	0.45	119	−0.01	10	6.4	*c-S*				Double optical nuclei?
NGC 7213	–	–	–	–	–	1.5	*S*	16.6	12.6	0.04	
NGC 7619	15.78	0.35	87	0.12	5	4.1	*c-S*				
NGC 7785	14.94	0.05	11	0.16	10	5.3	*c-S*				

Notes. Structural parameters from fits to the *V*-band major-axis surface brightness profiles (Appendix A, Figures 22 and 23). The superscript "+" is used to indicate that an *F*606*W* surface brightness profile is used, rather than an *F*555*W* surface brightness profile. Column 1: galaxy name. Columns 2–7: best-fit parameters from the core-Sérsic model, Equation (2). Column 8: indicates the profile classification where *c-S* = core galaxy described by the core-Sérsic model, and *S* = Sérsic galaxy described by the Sérsic model. Column 9: point-source apparent magnitude. Column 10: nuclear disk central surface brightness. Column 11: nuclear disk scale length. Column 12: description of inner additional light components. A "?" indicates a tentative classification.

4486B, 4552, and 4649) in common with Ferrarese et al. (2006) and Côté et al. (2006). While Trujillo et al. (2004) classified NGC 1700 as a Sérsic galaxy after fitting a profile sampled from $R \sim 0.''1$ to $70.''0$, we *tentatively* identify a small core within $R_b \sim 0.''07$. Apart from NGC 1700, our profile classifications are in agreement with Trujillo et al. (2004) and Ferrarese et al. (2006).

The break radii presented in Trujillo et al. (2004) agree with our values for all three "core" galaxies that we have in common. While four of the break radii from the six "core" galaxies in common with Ferrarese et al. (2006) agree with our values, NGC 4382 and NGC 4552 are discrepant (see Figure 5). As noted by Ferrarese et al. (2006, their Section 5.2), the outer disk in the peculiar S0 galaxy NGC 4382 can, if not modeled as a separate component when the data extends into the domain of the disk, bias (high) the Sérsic index that would otherwise be ascribed to the bulge of this galaxy. We have therefore modeled their extended light profile for NGC 4382 with a core-Sérsic plus outer exponential disk to show this. Our break radius, and Sérsic index (see Figure 6), differ from the values presented in Ferrarese et al. (2006) because this galaxy's outer disk did indeed bias their analysis (Figure 7). Modeling the light profile from Ferrarese et al. (2006) for NGC 4552, we recover their fit when using their published parameters but find that it can be substantially improved upon with a smaller break radii and a value of $\alpha = 2$ (Figures 22 and 7). This should be compared with Kormendy et al. (2009, their Figure 56), which reports a core radius in excess of 1 arcsec from their visual inspection. Having accounted for NGC 4382 and NGC 4552, Figure 5 reveals an excellent agreement between the break radii obtained

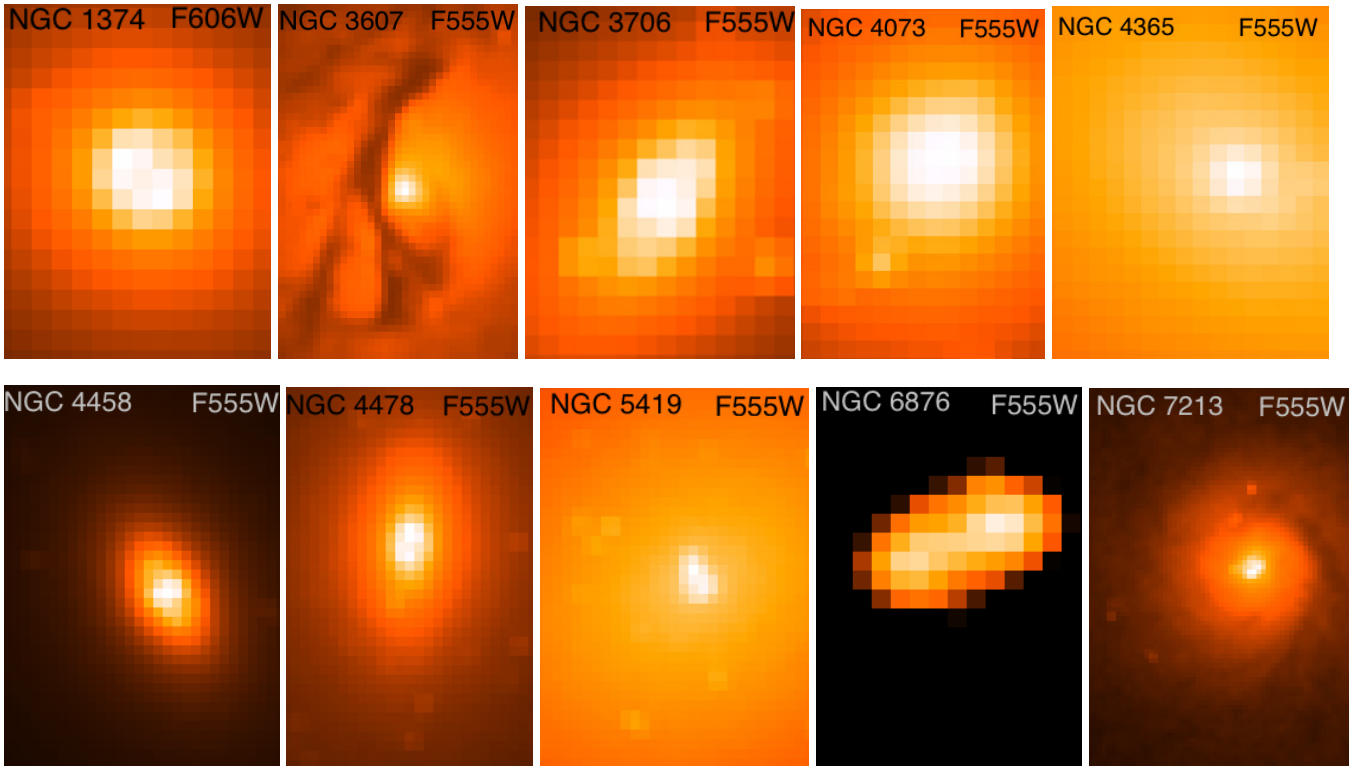

Figure 4. Optical *HST* images of galaxy centers. Each galaxy was observed using the high-resolution ($0\farcs046$ pixel^{-1}) PC1/WFPC2 camera.
(A color version of this figure is available in the online journal.)

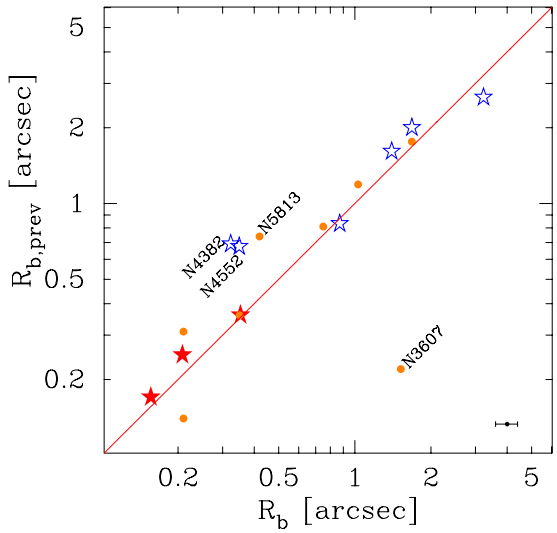

Figure 5. Comparison of the core-Sérsic model's break radii from this study (R_b: Table 2, *V* band) and previous break radii, $R_{b,\mathrm{prev}}$, from (i) Trujillo et al. (2004, *R* band, filled stars), (ii) Ferrarese et al. (2006, *g* band, open stars), and (iii) Richings et al. (2011, various bands, filled circles). We have converted the geometric-mean radii from Ferrarese et al. (2006) into semi-major axis radii using their ellipticity values. A representative error bar is shown at the bottom of the panel.
(A color version of this figure is available in the online journal.)

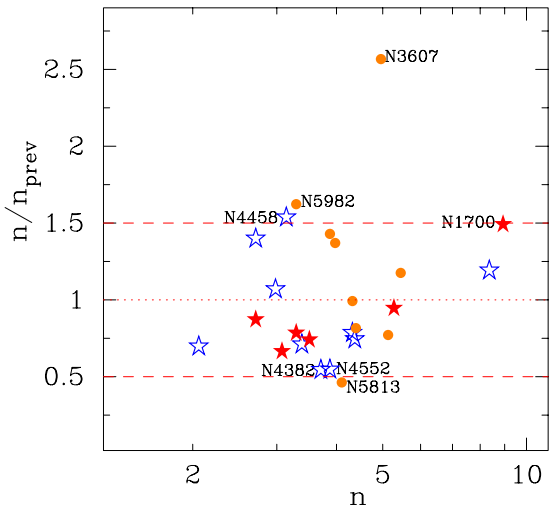

Figure 6. Comparison of our major-axis Sérsic indices, *n*, with previously published values (n_{prev}) derived using a greater radial extent. The filled stars and circles are major-axis Sérsic indices from Trujillo et al. (2004) and Richings et al. (2011), respectively, while the open stars are geometric-mean axis Sérsic indices from Ferrarese et al. (2006).
(A color version of this figure is available in the online journal.)

by us, Trujillo et al. (2004), and Ferrarese et al. (2006). Marginal discrepancies in the break radii may also arise because of the different filters used in each study. While we use data from the *F*555*W* filter, Trujillo et al. (2004) primarily used data from an *F*702*W* filter, and we have taken the *F*475*W* data, rather than the F850LP data, from Ferrarese et al. (2006) as it most closely matches our *F*555*W* data.

When the radial extent of one's data does not adequately probe the curvature of a spheroid's light profile, one may not recover the correct Sérsic index. Graham et al. (2003) noted that truncating a profile from $\sim$(2–3)R_e to $\sim$1 R_e changes the fit parameters by up to 5%. Concerned about this, as our data only extend to $10''$, we have additionally compared our Sérsic indices with those from Trujillo et al. (2004) and Ferrarese et al.

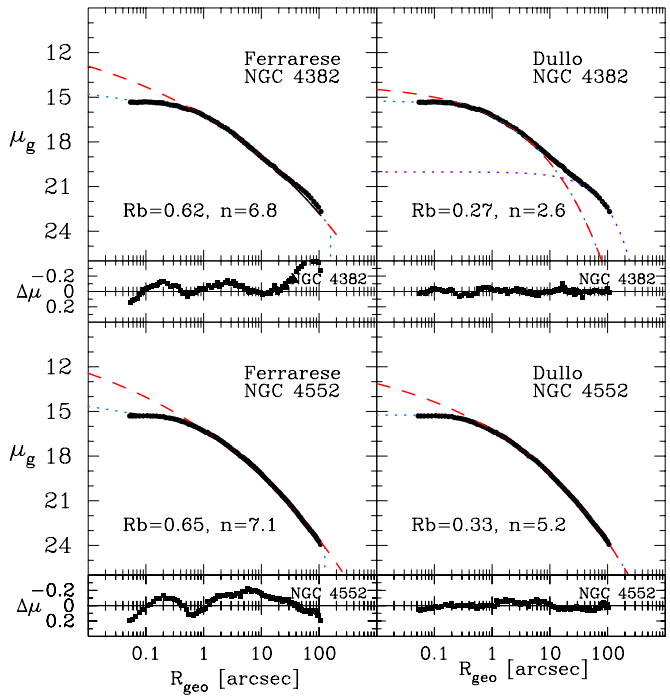

Figure 7. Left panels: core-Sérsic models presented in Ferrarese et al. (2006). Right panels: our modeling of their published profiles, including an outer exponential disk (dotted line) for NGC 4382. Note: while the innermost data points of the flat cores *are* slightly affected by the PSF, which we have not accounted for here and thus things look worse for the Ferrarese et al. fit than they are at small radii, this is not the reason for the different Sérsic indices and break radii. For the four other core-Sérsic galaxies that we have in common with Ferrarese et al. (2006), we agree on the location of the break radii (Figure 5).

(A color version of this figure is available in the online journal.)

(2006), which had a larger radial extent. First, we note that the Sérsic index for NGC 4458 from Trujillo et al. (2004) was biased (high) by the presence of a nuclear disk that was not separately modeled as we have done here. They noted that they were not confident in their analysis of this galaxy and as such we have excluded this one galaxy from Trujillo et al. (2004) in our Figure 6. With the exception of NGC 4552 and NGC 4382, mentioned in the preceding paragraph, the agreement between the Sérsic indices is good to within 50% or better, which is in fair agreement with the 1σ uncertainty range of $\pm 36\%$ found by Allen et al. (2006, their Figure 15). However, it should also be noted that due to ellipticity gradients, the major-, minor-, and geometric-mean axes do not have the same Sérsic index (Ferrari et al. 2004). Their values can disagree by up to a factor of ~ 2 (e.g., Caon et al. 1993, their Figure 4). Consequently, some of the scatter seen in Figure 6, which compares our major-axis Sérsic indices with the geometric-mean axis values from Ferrarese et al. (2006) is because of this.

We have also been able to include a comparison of break radii and Sérsic indices, in Figures 5 and 6, respectively, for eight core galaxies that we have in common with Richings et al. (2011). In general, the agreement is good, although there are three somewhat discrepant points. For NGC 5982, we suspect that Richings et al. may have missed the core with their Sérsic $n = 2$ fit to this large elliptical galaxy with $\sigma = 239$ km s^{-1} and $M_V = -22$ mag. We are also inclined to prefer our $n = 4$ core-Sérsic fit to NGC 5813 rather than the $n = 9$ core-Sérsic fit of Richings et al., which results in a larger apparent core. However, we suspect that the dust ring in NGC 3607, although subtracted, may have still interfered with the optical light profile from Lauer et al. (2005). As such, we feel that our break radius may be overestimated for this one galaxy, explaining its outlying nature in the central mass deficit versus black hole mass diagram (see Section 7.3).

Recently, Dhar & Williams (2011) noted that surface brightness profiles of elliptical galaxies can be modeled well using the multi-component DW function (Dhar & Williams 2010), with smaller rms residuals than the Sérsic, core-Sérsic, and Nuker models. Although we fit the profiles (from Lauer et al. 2005) with limited radial ranges, for galaxies that we have in common with Dhar & Williams (2011)—NGC 4365, NGC 4382, NGC 4406, NGC 4458, NGC 4472, NGC 4473, NGC 4478, NGC 4552, and NGC 4649—our rms residuals are smaller than those obtained with the DW function (Dhar & Williams 2011, their Table 1) except for NGC 4458 (Appendix A, Figure 22).

5. BREAK RADII MEASUREMENTS

Given that the core-Sérsic model and the Nuker model yield different core sizes, we have included an extended section on the measurement of the break radii via different methods.

5.1. The Nuker Model

As noted previously, the Nuker team (Lauer et al. 1995, 2005) used a five-parameter double power-law model for fitting the inner radial surface brightness profiles of galaxies. Dubbed the "Nuker law," it can be written as

$$I(R) = I_b 2^{(\beta-\gamma)/\alpha} \left(\frac{R}{R_b}\right)^{-\gamma} \left[1 + \left(\frac{R}{R_b}\right)^{\alpha}\right]^{(\gamma-\beta)/\alpha}, \quad (4)$$

where I_b is the intensity at the break radius R_b. The negative logarithmic slopes for the inner and outer power-law regions are denoted by γ and β, respectively, while α controls the sharpness of the transition. R_b represents both the radius of maximum curvature of this *model*, and the location where the local gradient of the model equals $-(\beta + \gamma)/2$. One can readily appreciate how fitting this model to a larger radial range, and thus to an increasingly steeper outermost region of what are curved surface brightness profiles, results in larger values of β and thus larger values of R_b. When this occurs, the value of α is also reduced, to accommodate an (artificially) increasingly broad transition. Having excluded additional nuclear components, Lauer et al. (2005) tabulated their best-fitting Nuker model parameters for the galaxies used in this study (see also Lauer et al. 2007a, 2007b) and we refer to those values in some of the following figures.

In their study of the nuclear regions of early-type galaxies, Rest et al. (2001) noted that for small values of α (i.e., broad transitions), the Nuker model's parameter γ is rather a representation of the slope of the brightness profile at radii much smaller than the image resolution limit. They therefore introduced another parameter, γ', that was the negative logarithmic slope of the Nuker model at $R = 0\farcs1$, and which was adopted by Lauer et al. (2005, 2007b). Graham et al. (2003) had however noted that because this local logarithmic slope γ' (at $R = 0\farcs1$) is a distance dependent quantity, galaxies with identical surface brightness profiles observed at different distances will have different γ' values. That is, this quantity is not a physically robust or meaningful quantity to use.

In Figure 8, we show how the γ values from the core-Sérsic model fit to 32 galaxies (having depleted cores relative to the outer Sérsic profile) compare with the γ (Pearson's

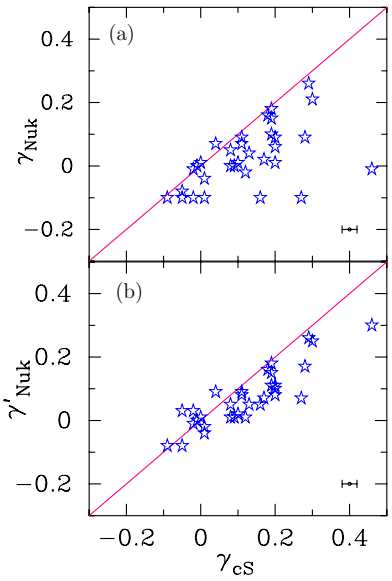

Figure 8. Comparison of the core-Sérsic model's inner negative logarithmic slopes (γ_{cS}, Table 2) with (a) the Nuker model's inner negative logarithmic slopes (γ_{Nuk}, from Lauer et al. 2005), and (b) the Nuker model's local negative logarithmic profile slope at the instrument resolution limit (γ'_{Nuk}, from Lauer et al. 2005). Representative error bars are shown at the bottom of each panel.

(A color version of this figure is available in the online journal.)

$r = 0.53$) and γ' (Pearson's $r = 0.87$) values obtained from the Nuker model. While the latter correlation coefficient is high, it is pointed out that this does not indicate a slope of unity, which would be required if the two parameters were equivalent. Instead, for positive values of γ_{cS}, the plots reveal that the Nuker model-derived values of γ'_{Nuk} and γ_{Nuk} are generally smaller than the core-Sérsic γ values.

5.2. Model Independent Approaches

5.2.1. $-d^2\ log\ I\ /\ d\ log\ R^2$= maximum

In an effort to obtain a non-parametric estimate of the break radii, we attempt to locate the radius corresponding to the maximum of the second derivative of the observed intensity profile in logarithmic coordinates, independent of any model or any smoothing or alteration of the data. In principle this model-independent radius should mark the break radius. In practice, however, Figure 9 reveals that there exists several comparable maxima over an extended radial range due to the sensitivity of this approach to the noise in the profile data. Therefore, we were unable to use this technique to acquire accurate break radii. We do however show in Figure 10 (right) that the core-Sérsic model's break radius corresponds to the radius where the second logarithmic derivative of this model has its maximum value.

In passing, we note that Lauer et al. (2007a, their Figure 17) and Lauer et al. (2007b, their Figure 16) had reported a strong consistency between their Nuker model break radii $R_{b,Nuk}$ and the location of the maximum of the second derivative of the intensity profile, in logarithmic coordinates, acquired from a model-independent approach. This claim was, however, surprising because it is well established and understood why $R_{b,Nuk}$ varies considerably as the fitted radial extent of a galaxy's surface brightness profile is varied (e.g., Graham et al. 2003, their Figures 2–4). As such, while the varying $R_{b,Nuk}$ always corresponds to the radius where the fitted Nuker model has the maximum of its second derivative, this typically will not correspond to the radius where the actual data have the

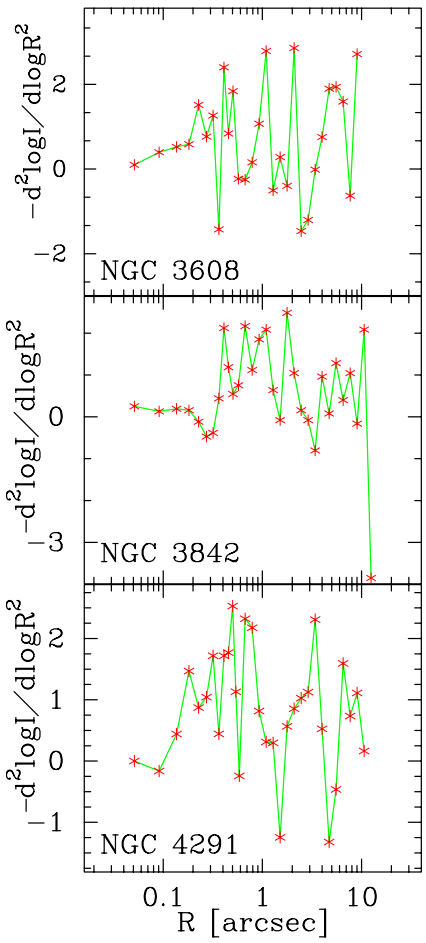

Figure 9. Typical examples of the second derivative of the surface brightness profile (in the *V* band) plotted against semi-major axis (see Section 5.2.1).

(A color version of this figure is available in the online journal.)

maximum in its second derivative. Using the same data as Lauer et al. (2007a, 2007b), we cannot reproduce their result. In Figure 9, we have shown that the second derivative of the observed galaxy brightness profiles has a large point-to-point variation. It is not clear how the result of Lauer et al. (2007a, 2007b) could be obtained without smoothing the data. Furthermore, we continue to reiterate the result of Graham et al. (2003), that the Nuker model fits, especially the break radius, are dependent on the chosen fitting range. In spite of this, that work was the sole basis for their rejection of the concerns about the Nuker model raised by Graham et al. (2003).

5.2.2. $-d\ log\ I\ /\ d\ log\ R = \gamma' = 1/2$

In a continued effort to better measure the sizes of partially depleted galaxy cores, in this section we investigate an alternative model-independent radius that has been used in the literature. This investigation is important if we are to accurately quantify the extent of damage caused by coalescing SMBHs at the centers of galaxies.

Most "core" galaxies have negative, logarithmic, inner profile slopes less steep than 0.3–0.5 (Glass et al. 2011, and references therein), before they transition to an outer Sérsic profile with a slope typically steeper than 0.5 (Lauer et al. 2005).[5] The negative logarithmic slope beyond the core, in the Sérsic portion of the

[5] As discussed by Graham & Guzmán (2003), pure "Sérsic" galaxies can also have inner profile slopes less steep than 0.5, and whether or not one measures

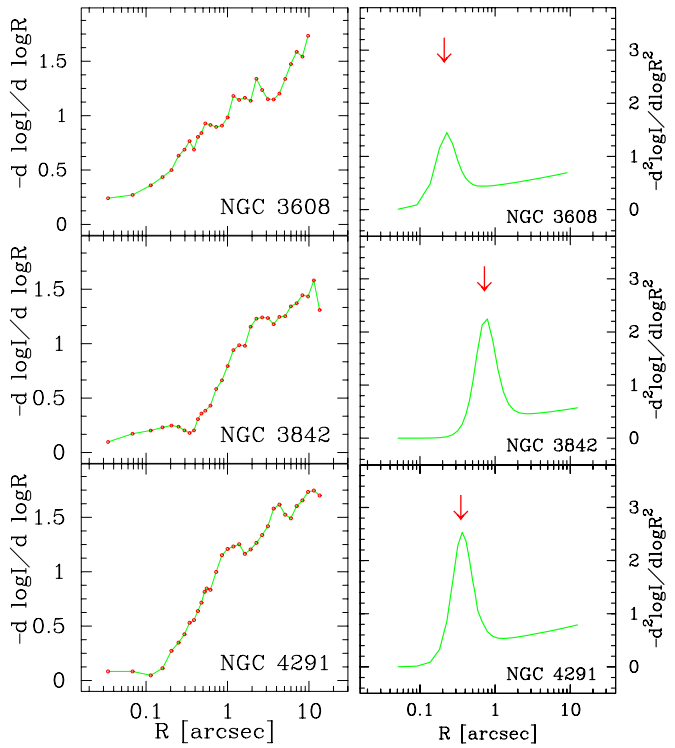

Figure 10. Left: typical examples of the negative logarithmic slopes of the surface brightness profile (in the V band) plotted against semi-major axis (see Section 5.2.2). Right: typical examples of the second logarithmic derivative of the fitted core-Sérsic model (in the V band) plotted against semi-major axis. Arrows indicate the break radii of the galaxies from the fitted core-Sérsic model (Table 2).

(A color version of this figure is available in the online journal.)

profile, varies as $(b_n/n)(R/R_e)^{1/n}$. Graham et al. (2003, their Figure 6) have revealed that this slope is steeper than 0.5 for Sérsic models with $n > 3$–4 once beyond 1% of the effective radius R_e. Given that Côté et al. (2007) have reported that cores extend to $\sim 0.02^{+0.025}_{-0.01} R_e$, we can appreciate why the slopes on the outer side of cores are steeper than 0.5. As such, the radius where the negative logarithmic slope of the underlying galaxy surface brightness profile γ' equals 1/2 (Carollo et al. 1997) can be used to find the transition radius between the inner core and the outer Sérsic profile, and thus approximate the break radius of the core-Sérsic model.

In finding the radius where $\gamma' = 1/2$, when present we avoided data points affected by central light excesses before applying this technique (Figure 10, left). We visually inspected individual profiles to double-check these objective break radii estimates and for (only) five galaxies (NGC 3607, NGC 3640, NGC 4406, NGC 4589, and NGC 5557) the data were too noisy; as such we excluded them from the comparison of break radii in the following subsection. The radii where $\gamma' = 1/2$ are plotted in Figure 11 and discussed in the following subsection.

Before proceeding, we note that Lauer et al. (2007a, p. 816) had also remarked that Carollo et al. (1997) had advocated use of $R_{\gamma'}$, with $\gamma' = 1/2$, as a core scale parameter. They wrote that "Since $R_{\gamma'=1/2}$ is generally well interior to $R_{b,\rm Nuk}$, it is not meant to describe the actual complete extent of the core; it is just a convenient representative scale." To reduce potential misinterpretation of this comment, it is important to note that

this (underneath any additional nuclear components) simply depends on how small one's R/R_e spatial resolution is (see Graham et al. 2003, their Figure 6).

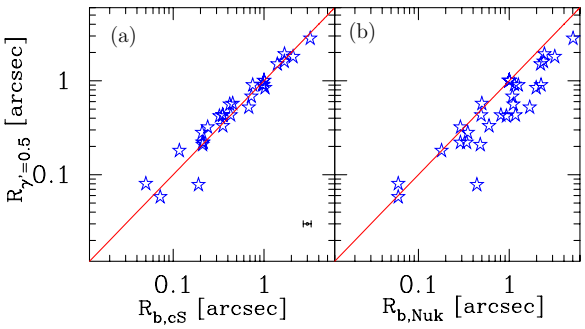

Figure 11. Comparison of $R_{\gamma'} = 1/2$ and (a) the break radius from the core-Sérsic model ($R_{b,\rm cS}$, see Table 2) and (b) the Nuker model ($R_{b,\rm Nuk}$; Lauer et al. 2005). When present, central light excesses are avoided when determining $R_{\gamma'=1/2}$. NGC 3607, NGC 3640, NGC 4406, NGC 4589, and NGC 5557 are excluded from this analysis due to considerable noise in their inner data. A representative error bar is shown at the bottom of panel (a).

(A color version of this figure is available in the online journal.)

the Nuker model's $R_{b,\rm Nuk}$ was also never meant to describe the complete extent of the core. While the published Nuker model break radii occur at large radii where the slope is steeper than −0.5 (see Figure 11(b)), the actual outer edge of the Nuker model's transition region occurs considerably further out than this, greater than both the Nuker model break radii and the outer edge of the core-Sérsic model. Moreover, due to the curved nature of the outer Sérsic profile, the outer edge of the Nuker model increases as the fitted radial extent is increased.

5.3. The Core-Sérsic Model

Figure 11(a) reveals a strong correlation (Pearson's $r = 0.96$) between the break radii estimated from the model-dependent (core-Sérsic) and the model-independent ($R_{\gamma'=1/2}$) quantitative analysis. One can similarly show that the negative logarithmic slope of the fitted core-Sérsic models has a value of 0.5 at a radius very close to the core-Sérsic model's break radius. This important result has not been noted before. Turning things around, this agreement endorses the use of $R_{\gamma'=1/2}$ when the data are not too noisy, albeit with the caveat that even galaxies without partially depleted cores may still have a resolvable radius where $\gamma' = 1/2$. The core-Sérsic model is therefore still recommended for identifying and quantifying cores.

For comparison, Figures 11(b) and 12 show that the measurement of the Nuker model's break radii presented in Lauer et al. (2007a, 2007b) against the model-independent break radii $R_{\gamma'=1/2}$ ($r = 0.91$) and the core-Sérsic break radii ($r = 0.90$). Graham et al. (2003) explained that increasing the fitted radial range of the Nuker model, into the curved profile beyond the core, will increase the slope of the Nuker model's outer power-law β and thus result in the Nuker model's break radius—corresponding to the location where the model's slope is the average of the inner and outer power-law slopes, γ and β—marching out to larger radii. For this reason, the Nuker model's break radius can be pulled out beyond the actual transition radius between the core and the outer Sérsic profile. On average, the Nuker break radii are ∼2 times bigger than the core-Sérsic break radii (Figure 13). While Lauer et al. (2007a, their Appendix C) refuted this criticism of the Nuker model, they simultaneously reiterated this very problem and subsequently used $R_{\gamma'=1/2}$. However they did not show how $R_{\gamma'=1/2}$ compared with the Nuker model break radii, which is done here for the present galaxy sample that have "real" cores (Figure 11(b)). The above problem with the Nuker model was, in part, the motivation for the core-Sérsic model.

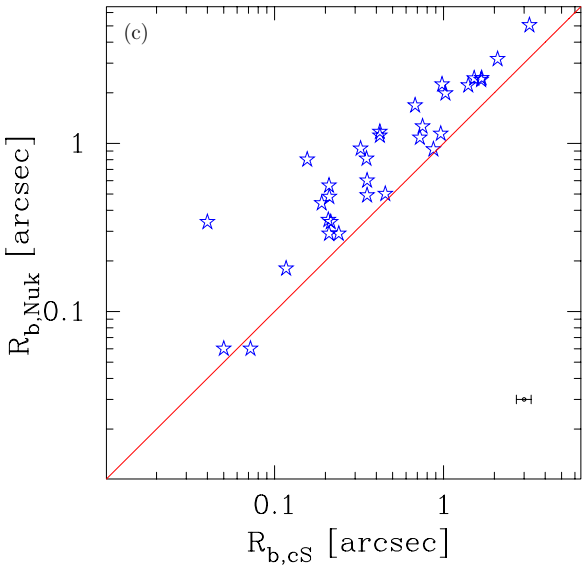

Figure 12. Comparison of the published Nuker break radii (Lauer et al. 2005) and the core-Sérsic break radii (see Table 2). A representative error bar is shown at the bottom of the panel.

(A color version of this figure is available in the online journal.)

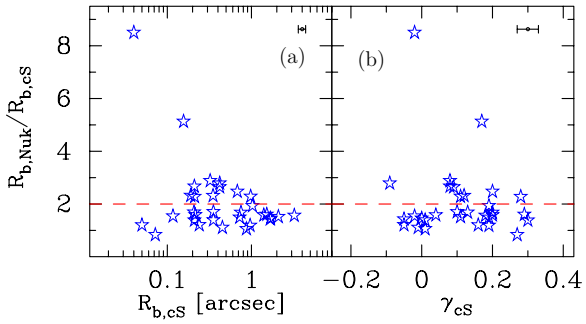

Figure 13. Ratio of the Nuker break radius ($R_{b,\rm Nuk}$; Lauer et al. 2005) to the core-Sérsic break radius ($R_{b,\rm cS}$, see Table 2) for core galaxies as a function of (a) $R_{b,\rm cS}$ and (b) the core-Sérsic model negative inner logarithmic slope $\gamma_{\rm cS}$.

(A color version of this figure is available in the online journal.)

Figure 13 reveals that there is no correlation between the ratio of the Nuker break radius ($R_{b,\rm Nuk}$) and the core-Sérsic break radius ($R_{b,\rm cS}$) with either (1) $R_{b,\rm cS}$ (Pearson coefficient $r = -0.29$, Figure 13(a)) or (2) the core-Sérsic negative inner logarithmic slope $\gamma_{\rm cS}$ (Pearson coefficient $r = -0.12$; Figure 13(b)).

From Table 1, we see that the break radii are smaller than 0.5 kpc. It would appear that the 500 pc resolution models by Martizzi et al. (2012, their Figure 7) may have "overcooked" core formation in their simulations of galaxies with cores up to ∼8–10 kpc in size. Similarly, the large ∼3 kpc cores created by Goerdt et al. (2010) are not observed in real galaxies.

6. IDENTIFICATION OF DEPLETED CORES, AND THEIR SLOPES

Initially, Kormendy et al. (1994) and Lauer et al. (1995) identified cores if the inner slope of the Nuker model was less than 0.3. Kormendy (1999, p. 124) subsequently relaxed this criteria to read "galaxies that show a break from steep outer profiles to shallow inner profiles," with the "outer profile" modeled by the outer power law of the Nuker model. However this definition of a core, and modeling of the stellar distribution, resulted in a disconnection with the curved outer Sérsic profile that was known to exist (e.g., Caon et al. 1993). Graham et al. (2003) therefore advocated that cores be identified and defined as a central stellar deficit relative to the outer Sérsic profile. Kormendy et al. (2009) quoted and partially embraced this new definition but opted to identify by eye the region to fit the Sérsic model and thus the onset of the break radius, rather than using the core-Sérsic model in an objective analysis. Their visual core classification agrees with our core identification, however, their approach resulted in break radii notably larger than those given by the core-Sérsic model (cf. Graham 2004; Ferrarese et al. 2006) and thus, given the results in the previous section, their break radii do not agree with the model-independent measurement of where the light profile has reached a steep outer profile with negative logarithmic slope equal to 0.5. This arose in part due to the lack of an infinitely sharp transition region. These larger break radii also result in larger estimates of the central mass deficit. Using a model-independent technique based on average profiles, Hopkins & Hernquist (2010) reported an upper limit to the mass deficit of 2–4 times the central black hole mass, in agreement with the analysis presented in Graham (2004) using the core-Sérsic model. This is in contrast to the values of 10–20 times the central black hole mass reported by Kormendy & Bender (2009).

Although all of the 39 galaxies in our sample were tabulated as "core" galaxies by the published analysis using the Nuker model (Lauer et al. 2005, their Table 4),[6] in Section 4 we effectively reclassified seven as Sérsic galaxies without partially depleted cores. This concern over misidentification in lower luminosity spheroids was first highlighted by Graham et al. (2003), and the discrepancy is fundamentally due to the inclusion of Sérisc galaxies with low Sérsic index n (and thus a shallow inner profile slope) that have no depleted core relative to the Sérsic profile, which describes the outer galaxy light distribution. The typical value of the Sérsic shape index (n) for the seven Sérsic galaxies is ≈3 (Figure 14).

In Figure 15, we have plotted the central surface brightness, $\mu_{0,V}$, of the galaxies or bulges obtained from the fitted models against their V-band absolute magnitude M_V. As with the M_V–n diagram (Figure 14), it is immediately apparent that the seven non-core galaxies are not some random sample from the 39 galaxies. They reside in a region of the M_V–$\mu_{0,V}$ diagram known to be occupied by galaxies without partially depleted cores.

Prior to Lauer et al. (2005), Trujillo et al. (2004) had already revealed that two of these seven galaxies (NGC 4458 and NGC 4478) had no partially depleted core. Ferrarese et al. (2006) additionally identified that NGC 4473 did not have a depleted core, and Kormendy et al. (2009) subsequently acknowledged that none of these three galaxies have depleted cores but instead have an excess of nuclear flux. In addition to the double-nucleus galaxy NGC 4486B, which is known to have a false core (Lauer et al. 1996), we find that NGC 1374, NGC 5576, and NGC 7213 also do not have cores depleted of stars relative to their host spheroid's (outer) Sérsic profile. NGC 7213 is a rather faint spiral galaxy with $M_B \sim -19.5$ mag and is thus not expected to have a depleted core like luminous, boxy spheroids do. NGC 1374 is also not a luminous galaxy; it too has $M_B \sim -19.5$ mag, and NGC 5576 is only 0.7 mag brighter.

Besides their distribution in Figures 14 and 15, it is of interest to examine whether there are additional characteristics among

[6] Although tabulated as having a "core" profile in Lauer et al. (2005), those authors are aware that NGC 4486B is not a "real" core galaxy (Lauer et al. 1996).

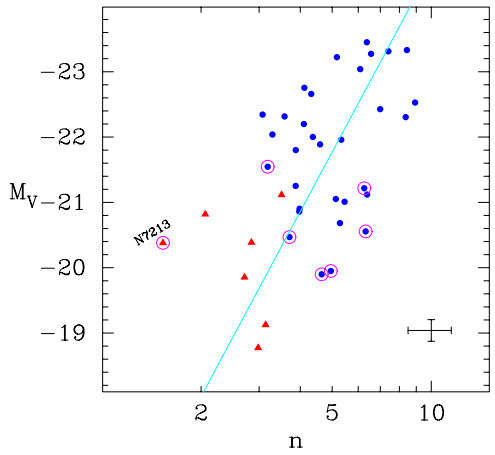

Figure 14. Absolute V-band galaxy magnitude from Table 1 (converted to bulge magnitude for the lenticular and spiral galaxies) plotted as a function of the Sérsic index, n, that quantifies the shape of the underlying galaxy or bulge, major-axis light profile. The line $M_B = -9.4\log(n) - 14.3$ is taken from Graham & Guzmán (2003, their Figure 10) and adjusted here to the V band using $B - V = 0.9$ (Fukugita et al. 1995). Filled circles are the core galaxies; filled triangles are the Sérsic galaxies; bulges are circled. The Pearson coefficient between M_V and n is $r = -0.34$. A representative error bar is shown at the bottom of the panel, but the 1σ uncertainty on the bulge magnitudes for disk galaxies is ∼0.75 mag.

(A color version of this figure is available in the online journal.)

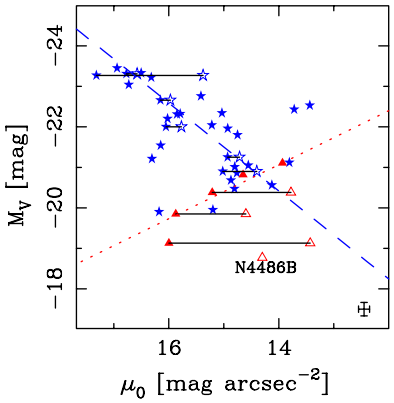

Figure 15. Absolute V-band magnitude of the galaxy (or the bulge of the disk galaxies) plotted against the core-Sérsic model's inner V-band surface brightness μ_0 at the instrument resolution limit $R = 0\farcs0455$ (excluding NGC 1374 and NGC 1399 for which there were no $F555W$ profiles). Filled stars and triangles are core-Sérsic and Sérsic galaxies, respectively. Galaxies with additional nuclear light have the host galaxy plus central excess flux, at $R = 0\farcs0455$, shown by the open symbols. Solid lines connect the central brightness values of the nucleated galaxies and their underlying host galaxies. The dotted line is taken from Graham & Guzmán (2003, their Figure 9) and adjusted here to the V band using $B - V = 0.9$. The dashed line, $M_V = -1.09(\mu_0 - 16.0) - 22.60$, shows our least-squares fit to the M_V and μ_0 relation for galaxies with "real" depleted cores, and having a Pearson's coefficient $r = -0.44$. A representative error bar is shown at the bottom of the panel, but the 1σ uncertainty on the bulge magnitudes for disk galaxies is ∼0.75 mag.

(A color version of this figure is available in the online journal.)

these seven galaxies, which have cores according to the Nuker model (Lauer et al. 2005) but do not have partially depleted cores relative to their outer Sérsic profile. From the full sample of 39 galaxies, nine have velocity dispersions $\sigma \leqslant 183$ km s^{-1} according to HyperLeda, and seven of these nine galaxies are the above Sérsic galaxies. Of the remaining two galaxies, NGC 3640 has $\sigma = 182$ km s^{-1} and a very small, questionable depleted core, and while NGC 4382 has $\sigma = 179$ km s^{-1} according to HyperLeda's mean value however the most recent measurement

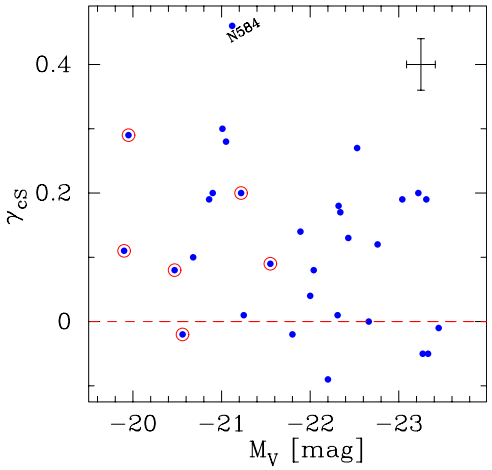

Figure 16. Comparison of the core-Sérsic model's negative inner logarithmic slope γ with the V-band absolute galaxy magnitude (bulge magnitude for disk galaxies). Bulges in disk galaxies are circled. A representative error bar is shown at the top of the panel, but the 1σ uncertainty on the bulge magnitudes for disk galaxies is ∼0.75 mag.

(A color version of this figure is available in the online journal.)

of $\sigma = 205 \pm 8$ km s^{-1} (Bernardi et al. 2002) is supportive of a "real" core.

Aside from the above mentioned confirmation by other authors, there are good reasons to suspect that the Nuker model struggles to identify cores that have been depleted relative to the inward extrapolation of the outer Sérsic profile in galaxies and bulges fainter than $M_V \approx -21$ mag (see Figure 14). While Lauer et al. (2007a) used their Nuker model parameters to determine where the fitted Nuker model has a slope of $-1/2$, which we consider to be a better measurement of the transition from a shallow core to a steep outer profile, one is left with the problem of not knowing which galaxies actually have depleted cores that are consistent with non-parametric identification methods, relative to the smooth inward extrapolation of the outer Sérsic profile. Figure 14 reveals that knowledge of this Sérsic index can help with this diagnosis, but it obviously requires remodeling the light profiles. An additional criterion, which could be better quantified with a larger galaxy sample, is that alleged cores in galaxies with $\sigma \leqslant 183$ km s^{-1} are likely not to correspond to a real deficit of stars.

Although our sample is not suitable for testing the bimodality, or lack thereof (Glass et al. 2011, and references therein), in the distribution of host galaxy central surface brightness slopes against absolute magnitude (which, for the reason we have just seen, cannot be used as a diagnostic of core identification), we do find that $\gamma \lesssim 0.3$ for all (core-Sérsic)-identified core galaxies, with the possible exception of only NGC 584 (where $\gamma = 0.46$; see Table 2, and Figure 16). The low-luminosity (low-n) Sérsic galaxies without cores can have inner slopes ranging from 0 to 0.5 and steeper depending on the radius where one samples the underlying host spheroid's Sérsic profile (Graham & Driver 2005, their Section 2.4). Figure 16 plots the relation between γ and the V-band absolute magnitude M_V for the *"true"* core galaxies given in Table 2. For the first time using the core-Sérsic model, we find that a number of bright (high-n) core galaxies exhibit values of γ less than 0 (see also Lauer et al. 2005, and references therein for galaxies with Nuker model values of $\gamma < 0$). Earlier studies with the core-Sérsic model had been confined to reporting $\gamma \gtrsim 0$. Kandrup et al. (2003) have discussed how black hole binaries may couple with the

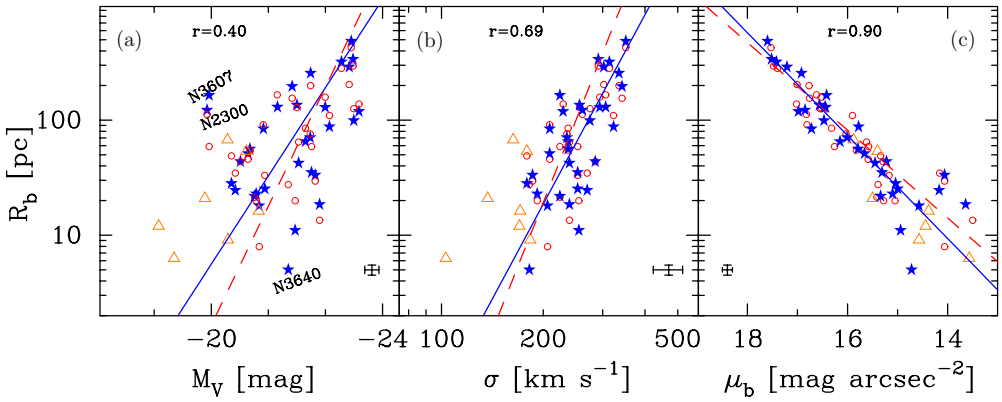

Figure 17. Core-Sérsic break radius and the published Nuker "cusp radius" $R_{\gamma'=1/2}$ (Lauer et al. 2007a), collectively R_b (in pc), are plotted as a function of (a) absolute V-band spheroid magnitude (Table 1), (b) central velocity dispersion σ (Table 1), and (c) the associated V-band surface brightness, collectively referred to as μ_b here (excluding NGC 1399 for which there was no $F555W$ profile). Filled stars are the core galaxies from this study fitted with the core-Sérsic model, while open circles are these same galaxies with R_b and μ_b ($\gamma' = 1/2$) data from Lauer et al. (2007a). Triangles show the location of the seven alleged "core" galaxies that are reclassified here as Sérsic galaxies and thus have no core-Sérsic break radii. The solid lines are least-squares fits to the core-Sérisc data, while the dashed lines are the published Nuker relations after they excluded galaxies with $M_V > -21$ mag (Lauer et al. 2007a, their Equations (13), (14), and (17)). Pearson correlation coefficients, r (and representative error bars), for our data are shown at the top (bottom) of each panel. For the disk galaxies, the 1σ uncertainty on the bulge magnitudes is $\sim$0.75 mag.
(A color version of this figure is available in the online journal.)

innermost stars and transport them to a larger radius, resulting in such surface brightness profiles.

7. STRUCTURAL PARAMETER RELATIONS

Having selected a set of cores based on the core-Sérsic model, we intend to obtain radial profiles over a greater radial extent for those 32 galaxies in a future paper. Figure 14 illustrates the linear correlation between the absolute galaxy magnitude (bulge magnitude in the case of disk galaxies) and the light-profile shape, n. As noted in Section 2, the bulge magnitude for the one spiral (Sa) and six lenticular (S0) galaxies in our sample are obtained using the representative bulge-to-disk flux ratio given in Graham & Worley (2008, their Table 5). Although our galaxies are limited in number and range of absolute magnitude (-18.77 mag $> M_V > -23.45$ mag), the overall distribution in the L–n diagram is in agreement with that from Caon et al. (1993), Graham & Guzmán (2003, their Figure 10), and Ferrarese et al. (2006). Given that the Sérsic index n is derived from 10″ profiles, we do not consider it to be as accurate as possible. Nonetheless, on average, the galaxy ensemble adhere to the established L–n relation, and are in fair agreement with the indices derived from fits to a larger radial extent (see Section 4.1). This gives us some confidence that our Sérsic parameters (which are only used once in this paper to derive a "ballpark" result in Section 7.3) are not too far off from the correct values.

7.1. R_b–L, R_b–σ, R_b–μ_b, μ_b–L, and μ_b–σ Relations

Building on earlier works that explored the connection between early-type galaxy dynamics and isophotal shape (e.g., Davies et al. 1983; Nieto & Bender 1989; Nieto et al. 1991), Faber et al. (1997) highlighted associations between the core structure and global galaxy properties. Bright ellipticals with boxy isophotes, slow rotation and pressure supported dynamics are "core" galaxies, while fainter elliptical galaxies with elliptical or "disky" isophotes and often rotational support are "Sérsic" ("power-law") galaxies. They went further to argue that the presence of a "core" is a better predictor of the slow rotation or boxiness than the galaxy absolute magnitude, although we have just learned that some of the Nuker-derived cores are not consistent with core-Sérsic cores or visual classification, i.e., they have been claimed to exist in galaxies with no depleted core. It would be remiss if we did not use our refined core-Sérsic parameters to derive updated scaling relations for galaxies that have central stellar deficits relative to their outer Sérsic profile. That is, we exclude those galaxies having no depleted cores.

Figures 17(a) and (b) display the relation between the core-Sérsic break radius (Table 2) and the published Nuker "cusp radius" $R_{\gamma'=1/2}$ (Lauer et al. 2007a), collectively R_b, and (1) the V-band absolute magnitude M_V listed in Table 1, and (2) the central velocity dispersion σ (Table 1). Using the ordinary least-squares (OLS) bisector regression (Feigelson & Babu 1992), a fit to the core-Sérsic R_b and σ yields

$$\log\left(\frac{R_b}{\mathrm{pc}}\right) = (5.47 \pm 0.68)\log\left(\frac{\sigma}{200\ \mathrm{km\ s^{-1}}}\right) + (1.27 \pm 0.11), \quad (5)$$

and further application of the bisector regression gives the relation between the core-Sérsic R_b and M_V as

$$\log\left(\frac{R_b}{\mathrm{pc}}\right) = (-0.58 \pm 0.09)(M_V + 22) + (1.90 \pm 0.10). \quad (6)$$

Similar trends between break radius and galaxy magnitude were also seen in Faber et al. (1997, their Figure 4), Ravindranath et al. (2001, their Figures 5(a) and (b)), Laine et al. (2003, their Figure 9), Trujillo et al. (2004, their Figure 9), de Ruiter et al. (2005, their Figure 8), and Lauer et al. (2007a, their Figure 19, bottom panel). The three outliers in our R_b–M_V relation are: NGC 2300 and NGC 3607—lenticular (S0) galaxies with a big core for their bulge brightnesses—and NGC 3640, a galaxy known for its morphological peculiarity, which probably signals an ongoing or a recent merger (Michard & Prugniel 2004). Shown in Figure 17(c) is R_b (core-Sérsic break radius from Table 2 plus Nuker "cusp radius" from Lauer et al. 2007a) as a function of μ_b (the V-band surface brightness at the core-Sérsic break radius and the Nuker "cusp radius", from Table 2 and Lauer et al. 2007a, respectively). The bisector fit to the core-Sérsic R_b and μ_b gives

$$\log\left(\frac{R_b}{\mathrm{pc}}\right) = (0.45 \pm 0.05)(\mu_b - 16) + (1.87 \pm 0.04), \quad (7)$$

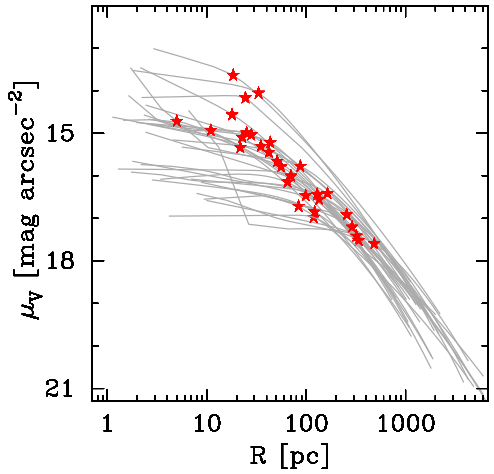

Figure 18. Compilation of the core-Sérsic fits to the major-axis surface brightness profiles of all core galaxies from Table 2 except for NGC 1399 for which there was only an *F606W* profile. Stars indicate the break radius of the individual profiles (cf. Figure 17(c)).

(A color version of this figure is available in the online journal.)

or

$$\mu_b = (2.24 \pm 0.28)\log\left(\frac{R_b}{100\ \mathrm{pc}}\right) + (16.30 \pm 0.06). \quad (8)$$

Equations (5), (6), and (8) update the R_b–σ, R_b–L, and μ_b–R_b relations presented in Lauer et al. (2007a, their Equations (13), (14), and (17), respectively). Figures 17(c) and 18 confirm, but re-define the tight correlation between the core-Sérsic core brightness μ_b and the core-Sérsic core radius R_b (Faber et al. 1997;[7] de Ruiter et al. 2005, their Figure 7; Lauer et al. 2007a, their Figure 6). Apparent in Figure 18 is a roughly universal profile beyond the core of "core" galaxies, out to ∼1 kpc, which explains the tight relation seen in Figure 17(c).

Figure 19(c) plots the core-Sérsic μ_b versus the Nuker μ_b. In overestimating the core radii, where $\gamma' \approx 1/2$, the Nuker model underestimates the associated surface brightness, by typically 1 mag arcsec^{-2} and up to 2 mag arcsec^{-2} with respect to the core-Sérsic model. In Figures 19(a) and (b), we show relations involving μ_b (the *V*-band surface brightness at the core-Sérsic break radius and the Nuker "cusp radius," from Table 2 and Lauer et al. 2007a, respectively) with M_V and σ. Akin to Figure 17(a), the (core-Sérsic)-identified core galaxies display a correlation between the core-Sérsic μ_b and M_V, such that the OLS bisector regression analysis gives

$$\mu_b = (-1.02 \pm 0.10)(M_V + 22) + (16.00 \pm 0.20). \quad (9)$$

The OLS bisector fit to the core-Sérsic μ_b and σ yields

$$\mu_b = (11.61 \pm 1.60)\log\left(\frac{\sigma}{200\ \mathrm{km\ s^{-1}}}\right) + (14.75 \pm 0.24). \quad (10)$$

7.2. Core Size versus Black Hole Mass

Although the relation between the break radius and the SMBH mass is less fundamental than the relation between the central mass deficit and the SMBH mass (e.g., Graham 2004; Ferrarese et al. 2006; Merritt 2006), de Ruiter et al. (2005) and Lauer et al. (2007a) nonetheless argue for the existence of a good correlation between the former. Shown in Figure 20 is the core-Sérsic break radius plotted against the black hole mass $M_{\rm BH}$ for eight core galaxies with direct black hole mass measurements (see Graham 2008b and Graham et al. 2011). The bisector fit to R_b and $M_{\rm BH}$ for these eight galaxies gives

$$\log\left(\frac{R_b}{\mathrm{pc}}\right) = (0.63 \pm 1.73)\log\left(\frac{M_{\rm BH}}{10^9\ M_\odot}\right) + (2.03 \pm 0.78). \quad (11)$$

However, while considering only seven of the eight core galaxies, after excluding the only disk galaxy (NGC 3607), the regression analysis of R_b and $M_{\rm BH}$ yields the more certain relation

$$\log\left(\frac{R_b}{\mathrm{pc}}\right) = (1.01 \pm 0.69)\log\left(\frac{M_{\rm BH}}{10^9\ M_\odot}\right) + (2.07 \pm 0.33). \quad (12)$$

[7] Faber et al. (1997) ascribed the tight correlation among the central properties of early-type galaxies to the presence of a "core fundamental plane" ($\log r_b$, μ_b, and $\log\sigma$), which is analogous to the global fundamental plane—$\log r_e$, μ_e, and $\log\sigma$ (e.g., Djorgovski & Davis 1987).

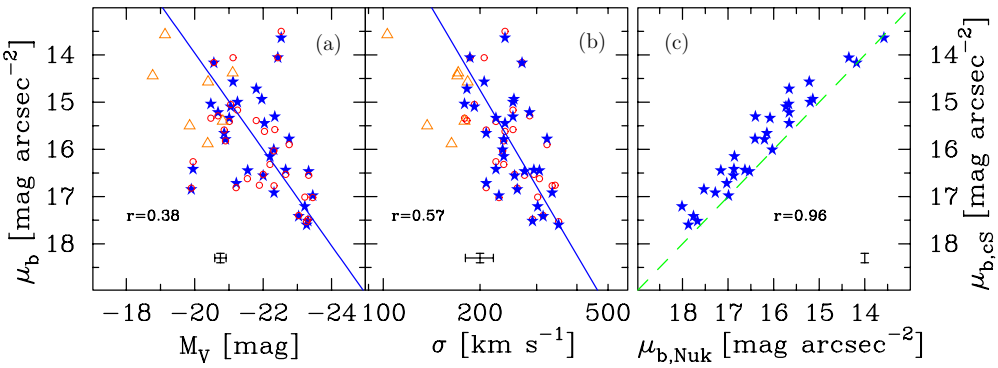

Figure 19. Core-Sérsic model's break surface brightness and the published Nuker's "cusp" surface brightness, collectively μ_b (*V* band), are plotted against (a) the absolute *V*-band magnitude of the galaxy (or the bulge for disk galaxies) and (b) the central velocity dispersion σ (see Table 1). Panel (c) plots the core-Sérsic $\mu_{b,\rm cS}$ against the published Nuker model's estimate of $\mu_{b,\rm Nuk}$ (Lauer et al. 2007b). Filled stars are the core galaxies from this study, while open circles are these same galaxies with R_b and μ_b from Lauer et al. (2007a). Triangles denote the seven Nuker "core" galaxies that are reclassified here as Sérsic galaxies. The solid lines (in panels (a) and (b), which correspond to Equations (9) and (10), respectively) are the least-squares fits to the μ_b–L and μ_b–σ core-Sérsic data. Pearson correlation coefficients, *r*, and representative error bars, for our data, are shown at the bottom each panel. For the disk galaxies, the 1σ uncertainty on the bulge magnitudes is ∼0.75 mag.

(A color version of this figure is available in the online journal.)

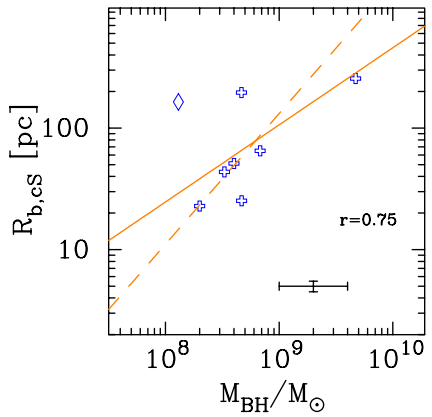

Figure 20. Core-Sérsic break radius $R_{b,cS}$ (Table 2) plotted as a function of the black hole mass M_{BH} for eight core galaxies with direct black hole mass measurements, obtained from Graham (2008b) and Graham et al. (2011) and adjusted to distances given in Table 1. The solid line (Equation (11)) is a least-squares fit to all eight core galaxies, while the dashed line (Equation (12)) is a least-squares fit to the seven core elliptical galaxies (open crosses) after excluding the only lenticular galaxy NGC 3607 (open diamond) having a Pearson correlation coefficient $r = 0.75$ as shown in the plot. A representative error bar is shown at the bottom of the panel (see the text for details).

(A color version of this figure is available in the online journal.)

Given the two widely used black hole mass estimators, the M_{BH}–σ relation (Ferrarese & Merritt 2000; Gebhardt et al. 2000) and the M_{BH}–L relation (Marconi & Hunt 2003), we can construct the R_b–M_{BH} relation from the R_b–σ and R_b–L relations in Section 7.1 to further investigate the core size and black hole connection. Combining the M_{BH}–σ relation from Graham et al. (2011, their final entry in Table 2, acquired using only elliptical galaxies) with the R_b–σ relation (Equation (5)) we can derive the new R_b–M_{BH} relation

$$\log\left(\frac{R_b}{\mathrm{pc}}\right) = (1.03 \pm 0.20)\log\left(\frac{M_{BH}}{10^9\,M_\odot}\right) + (2.08 \pm 0.22), \quad (13)$$

which is in remarkable agreement with Equation (12). Combining the R_b–L relation (Equation (6)) with the M_{BH}–L relation for predominantly massive spheroids from Graham (2007, his Equation (19)) converted to the V band using $B - V = 0.9$ (Fukugita et al. 1995), yields

$$\log\left(\frac{R_b}{\mathrm{pc}}\right) = (1.45 \pm 0.29)\log\left(\frac{M_{BH}}{10^9\,M_\odot}\right) + (2.03 \pm 0.16). \quad (14)$$

While the M_{bh}–L relation is likely to be non-log-linear, Graham (2012b), the log-linear relation presented by Graham (2007) is dominated by massive spheroids and thus a good representation of the M_{BH}–L relation for the "core" galaxies.

It is worth noting that the scatter in the direct R_b–M_{BH} relation established using the seven elliptical core galaxies with direct black hole mass measurements (Equation (12)) is large. Although we only have a limited number of galaxies with a measured black hole mass and Equation (12) is somewhat driven by the highest mass black hole,[8] Equation (12) is consistent (overlapping error bars) with the two inferred relations (Equations (13) and (14)). Moreover, in contrast to the discussion in Lauer et al. (2007a, their Equations (20) and (21)), there is a good consistency among the deduced relations (Equations (13) and (14)). The updated relations are not (1) contaminated by the inclusion of galaxies without cores nor (2) based on galaxy rather than bulge luminosity for the disk galaxies (an issue discussed by Graham 2008a, his Section 6), and (3) use core-Sérsic break radii.

[8] Removing the highest mass black hole and excluding the disk galaxy gives a slope of 1.63 ± 0.75.

7.3. Central Mass Deficit

Galaxy merging is believed to be a common occurrence, responsible for the morphologies of elliptical galaxies. Growing evidence, based on extensive numerical experiment has indicated that the merger remnant of collisions between nearly equal mass spiral galaxies resemble early-type galaxies (e.g., Toomre & Toomre 1972; Hernquist 1993; Somerville & Primack 1999; Cox et al. 2006; Naab et al. 2006; Naab & Ostriker 2009). "Dry" mergers of elliptical galaxies may subsequently build "core" galaxies (e.g., Faber et al. 1997; Khochfar & Burkert 2003).

In "core" galaxies, the inner most stars are thought to have been ejected by inwardly spiraling binary SMBHs in the course of such dry, i.e., dissipationless, galaxy mergers, producing the observed central luminosity deficit, L_{def}, relative to the inward extrapolation of the outer Sérsic profile. Multiplying this deficit by the appropriate stellar mass-to-light ratio gives the central mass deficit, M_{def}. More specifically, scattering of stars from the galactic nuclei in three-body interactions (since there is no significant amount of gas that may render dynamical friction) is thought to be the avenue through which the coalescing binary black holes will "harden" and be delivered to the galaxy center (e.g., Begelman et al. 1980; Nakano & Makino 1999; Milosavljević & Merritt 2001). Using N-body simulations, Merritt (2006) showed that core formation is a cumulative process, where the total central mass deficit after N dry mergers is such that $M_{def} \approx 0.5 N M_{BH}$. Gualandris & Merritt (2012) further discuss the long-term evolution of black hole binaries affecting the central stellar distribution, and scouring out cores having radii bigger than the influence of the binaries.

Here, we have (1) identified the galaxies with scoured out "cores" (Table 2) and (2) quantified how their sizes scale with the final black hole mass M_{BH} (Section 7.2). Graham's (2004) estimation of the central stellar mass deficit (M_{def}) through the employment of the core-Sérsic model yielded $M_{def} \approx M_{BH}$, a result later confirmed by Ferrarese et al. (2006). This mass deficit is in accord with hierarchical galaxy formation models, where luminous galaxies are a by-product of about one to two major dissipationless merger. For reference, based on observations of galaxy pairs, Xu et al. (2012) found that since $z = 1$, massive galaxies have experienced 0.4 to 1.2 major mergers (see also Bell et al. 2004).

In Figure 21, we present tentative central stellar mass deficits obtained using our core-Sérsic model parameters and Equation (A19) from Trujillo et al. (2004) plotted against the observed or predicted (Graham et al. 2011) SMBH mass for each core galaxy. While R_b, μ_b, and γ are well constrained from our core-Sérsic fits, R_e and n may be less well constrained (Section 4.1) and as such we caution about overinterpreting the results in Figure 21. In passing, we again note that the break radius and mass deficit for NGC 3607 may be too large, based on *HST*/NIC2 data analyzed by Richings et al. (2011). Here, we simply remark that the mass deficits scatter around 0.5 to 4 times the central SMBH mass. M_{def}/M_{BH} ratios less than 0.5 imply that a minor-merger event may have taken place (in the absence of loss cone refilling). Note that we follow Graham (2004) and

Table 3
Comparison of the Detection of Nuclear Components from Different Studies

Galaxy	Profile Type	Rest et al. (2001)	Ravindranath et al. (2001)	Lauer et al. (2005)	Côté et al. (2006)	Our Result
NGC 0741	*c-S*	...	...	Yes	...	Yes
NGC 1374	*S*	...	...	No	...	Yes
NGC 1399	*c-S*	...	...	Yes	...	No
NGC 4278	*c-S*	...	Yes	Yes	...	Yes
NGC 4365	*c-S*	No	...	Yes	Yes	Yes
NGC 4406	*c-S*	...	No	Yes	No	No
NGC 4458	*S*	...	...	No	Yes	Yes
NGC 4472	*c-S*	...	No	Yes	No	Yes
NGC 4478	*S*	No		Yes	Possibly	Yes
NGC 4486B	*S*	...	...	No	Possibly	Possibly
NGC 4552	*c-S*	...	...	Yes	No	Yes
NGC 5419	*c-S*	...	...	Yes	...	Yes
NGC 6876	*c-S*	...	...	No	...	Possibly
NGC 7213	*S*	...	...	Yes	...	Yes

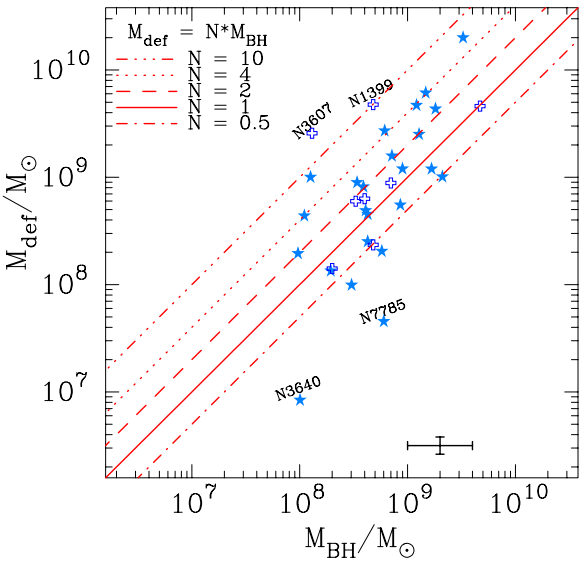

Figure 21. Tentative central mass deficit ($M_{\rm def}$) vs. black hole mass ($M_{\rm BH}$) for 32 core galaxies. We used Graham (2008b) and Graham et al. (2011) for direct supermassive black hole (SMBH) mass measurements of eight core galaxies (open crosses), while the M–σ relation presented in Graham et al. (2011) was used for estimating the SMBH masses of the remaining 24 core galaxies (filled stars). A representative error bar is shown at the bottom of the panel.

(A color version of this figure is available in the online journal.)

assume a V-band stellar mass-to-light ratio of ∼3.5 (Worthey 1994) to compute the mass deficits. For further reference, using N-body simulations, Kulkarni & Loeb (2012) measure mass deficits that are up to five times the mass of the central black hole.

Lauer et al. (2007a) proposed an alternate method to quantify the central stellar mass deficit in terms of a core with zero transition region breaking to an outer power-law profile with negative, logarithmic slope β. However, as revealed by Graham et al. (2003), the Nuker model β is not a robust quantity but varies with the radial range of the light profile that one tries to model. The range of mass deficit-to-black hole mass values in Figure 21 is notably less than the values in Lauer et al. (2007a), which were as high as ∼19 at $M_{\rm BH} = 10^9\,M_\odot$ (for black hole masses predicted using their $M_{\rm BH}$–σ relation). Kormendy et al. (2009, their Figure 42) also reported central mass deficits that were some ∼5 to 20 times greater than the central black hole mass, raising further doubts over their method of analyzing the galaxy light profiles (see the model-independent analysis by Hopkins & Hernquist 2010).

Finally, using Nuker model parameters, Gültekin et al. (2011) report a break radius of 0.″93 for NGC 4382 and a central mass deficit of $5.9 \times 10^8\,M_\odot$. Our analysis yields a break radius roughly three times smaller (0.″32) and a central mass deficit that is also three times smaller ($1.8 \times 10^8\,M_\odot$).

Having refined the core galaxy sample in this study, in a follow-up paper we intend to acquire a greater radial range of the light profiles for these galaxies, enabling a better estimate of the outer Sérsic parameters and thus the central mass deficits. This will allow us to check for a positive $M_{\rm def}/M_{\rm BH}$ correlation with host spheroid mass and $M_{\rm BH}$, tentatively seen in Figure 21.

8. ADDITIONAL NUCLEAR COMPONENTS

Additional nuclear light is detected in 12 (∼31%) of the 39 galaxies. Table 3 presents a comparison of detections of additional nuclear components from different studies; as done by Côté et al. (2006, their Table 3). Although the majority of our sample are core galaxies (∼82%), 5 of the 12 nucleated galaxies are Sérsic galaxies. We find good agreement with the work of Côté et al. (2006) in assigning the additional nuclear components with only two exceptions (NGC 4472 and NGC 4552). NGC 4552 has a point-source AGN (Renzini et al. 1995; Carollo et al. 1997; Cappellari et al. 1999) with a radio flux ∼103 mJy at 1.4 GHz (Condon et al. 1998). As for the Sy2 galaxy NGC 4472, at odds with Lauer et al. (2005) but in agreement with Côté et al. (2006), Ravindranath et al. (2001) also did not detect any additional nuclear component (Soldatenkov et al. 2003). We do however note that this galaxy's apparent point source (which has a radio flux ∼752 mJy at 1.4 GHz; White & Becker 1992) is very faint and the presence of dust can lead to such small irregularities in profiles acquired after image deconvolution.

Lauer et al. (2005) identified the nuclear light excess as a central upward deviation from the best Nuker model fit to the host galaxy surface brightness profile. Their identification is not always consistent with our analysis. The relative faintness and extended nature of the additional nuclear components in NGC 1374 and NGC 4458 are viable explanations as to why our detections are at odds with Lauer et al. (2005). We also do not detect additional nuclear light in our data for NGC 1399 nor NGC 4406. Ravindranath et al. (2001) and Côté et al. (2006) also

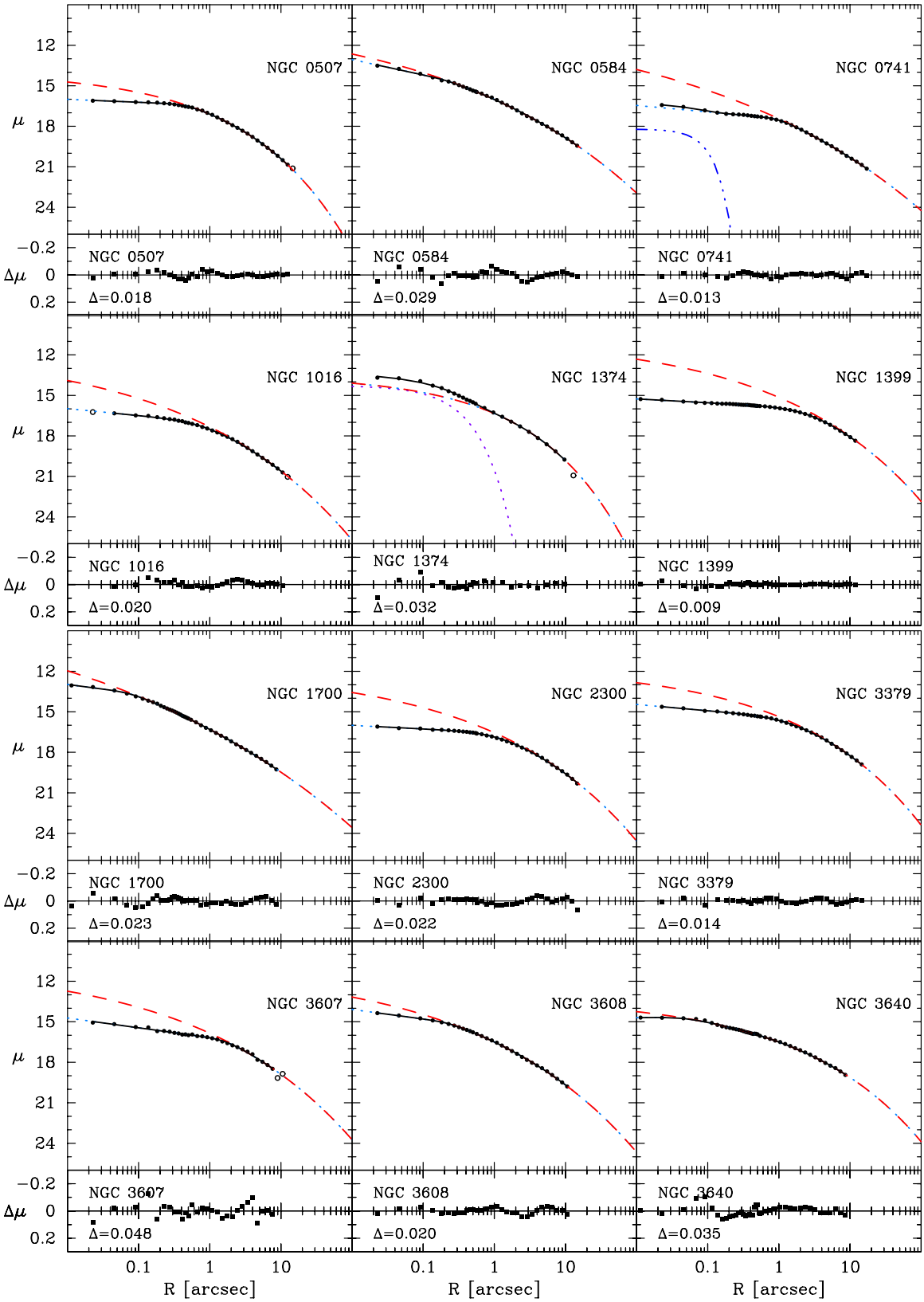

Figure 22. Major-axis surface brightness profiles for the galaxies listed in Table 1. All profiles were obtained with the *F*555*W* (∼*V*-band) filter, except for NGC 1374 and NGC 1399, which were obtained with the *F*606*W* (∼*R*-band) filter. The dashed curves show the Sérsic component of the core-Sérsic fits to the data, while additional nuclear sources were fit with either a Gaussian (dash-dot-dot-dot curve) or an exponential function (dotted curve). The solid curves show the complete fit to the profiles, with the rms residuals, Δ, about each fit given in the lower panels. Data points excluded from the fits are shown by the open circles. Brief details on NGC 1374, NGC 3607, and NGC 3640 are provided in Appendix B (see also the text).

(A color version of this figure is available in the online journal.)

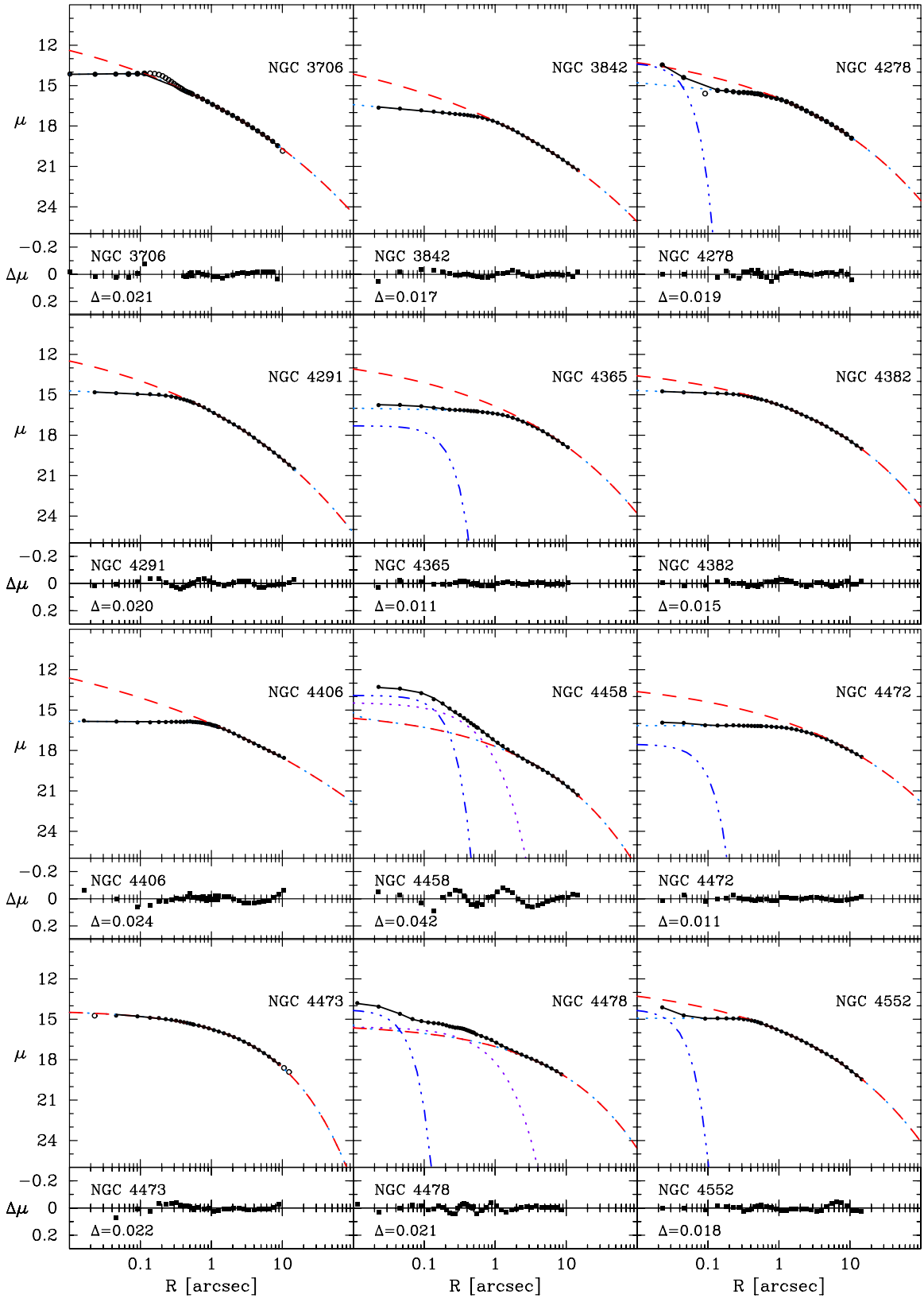

Figure 22 (Continued)

noted the absence of central light excess in NGC 4406, while Gebhardt et al. (2007) have also reported that NGC 1399 lacks any second component. Lyubenova et al. (2008) do however provide tentative evidence for the existence of a nuclear star cluster (or swallowed globular cluster) in NGC 1399. Lastly, Rest et al. (2001), after adopting a conservative central nuclei assigning approach reported the absence of additional nuclear components in NGC 4365 and NGC 4478, while all successive

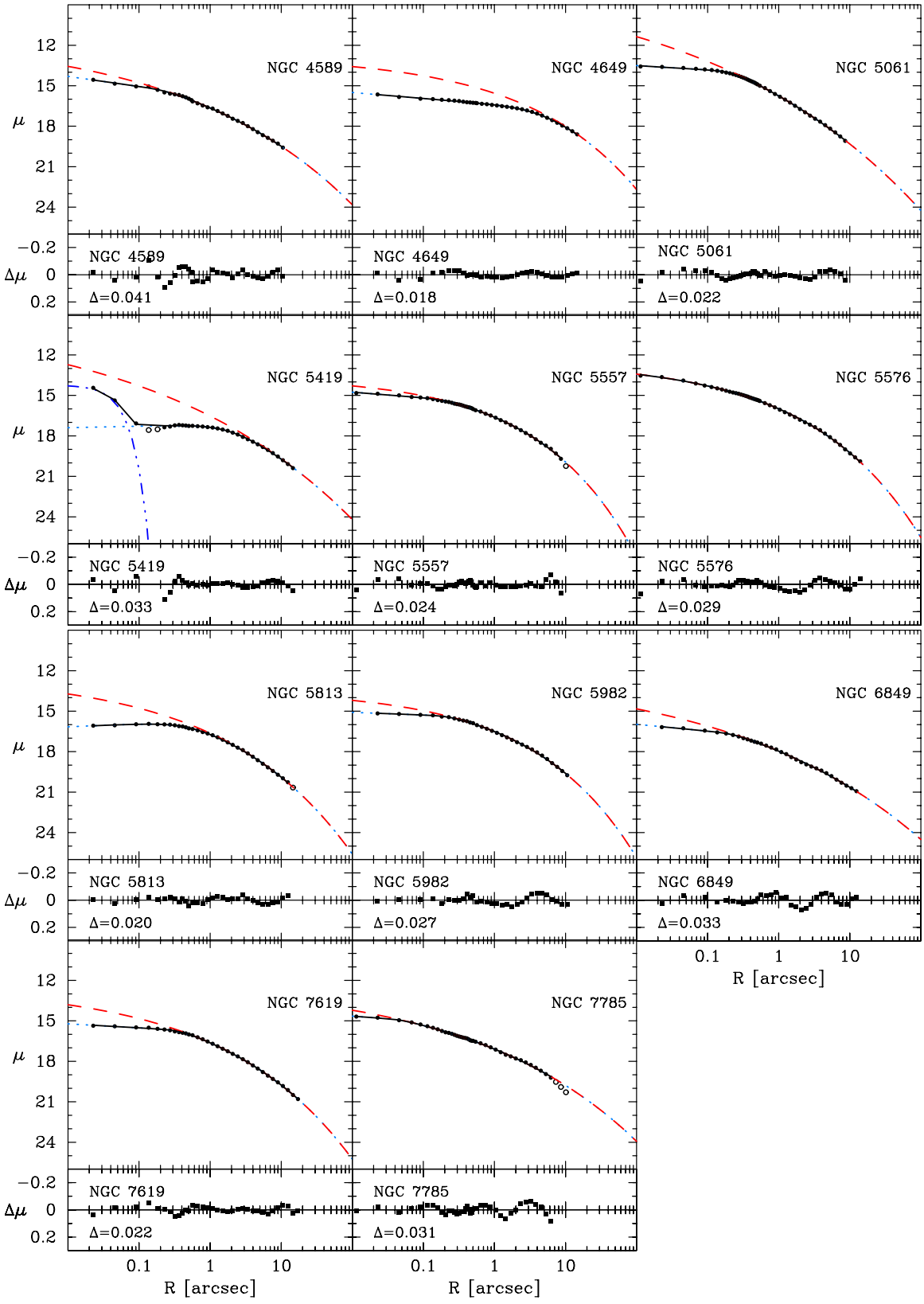

Figure 22 (Continued)

studies, including ours, identified central light excess in these two galaxies.

Of the five Sérsic galaxies with an additional nuclear component, only one, NGC 7213 (Véron-Cetty & Véron 1988), has a central light excess associated with nonthermal emission from an AGN. We further note that the remaining four nucleated Sérsic galaxies have a nuclear disk, a non-AGN central nuclei, or both. In contrast, we note the presence of AGN in (at

least) five of the seven nucleated core galaxies: NGC 741 (Condon et al. 2002), NGC 4278 (Younes et al. 2010), NGC 4472 (Diehl & Statler 2008), NGC 4552 (Carollo et al. 1997; Cappellari et al. 1999), and NGC 5419 (Capetti & Balmaverde 2005). Such prevalence is in accord with the studies by Balmaverde & Capetti (2006) and Richings et al. (2011; see also Pellegrini 2010). The central light excess in the remaining two core galaxies is not AGN related: NGC 4365 has a stellar cluster (Carollo et al. 1997) and NGC 6876 has a double optical nucleus possibly from an inclined disk (Lauer et al. 2002).

9. CONCLUSIONS

We have re-modeled the major-axis, surface brightness profiles of 39 alleged "core" galaxies from Lauer et al. (2005), using Sérsic and core-Sérsic models. We have additionally and simultaneously accounted for the point sources and additional nuclear components that were excluded by the Nuker analysis. Consistent with earlier published works, we found that the Sérsic and core-Sérsic models yield a robust representation of the underlying light distributions of Sérsic and core-Sérsic galaxies, respectively, all the way to the resolution limit. The typical rms residual scatter is 0.02 mag arcsec^{-2}.

The main results of this work are as follows.

1. We have identified 7 of the 39 "core" galaxies from Lauer et al. (2005) to be Sérsic galaxies that do not have partially depleted cores relative to the inward extrapolation of their outer Sérsic light profile. This situation tends to arise in galaxies and bulges fainter than $M_V \approx -21$ mag. Such galaxies with spheroid Sérsic index $n \lesssim 3$ or velocity dispersion $\sigma \lesssim 183$ km s^{-1} are not likely to have partially depleted stellar cores.
2. We provide physical parameters (R_b, μ_b, γ) for the cores of 32 "core" galaxies, derived using the core-Sérsic model.
3. Due to noise or real small-scale structure, non-parametric core size estimations obtained by locating the maximum of the second logarithmic derivative of the (non-smoothed) light profile, i.e., the point of greatest curvature, appear to be unreliable (Figure 9).
4. As with the Nuker model, the break radius of the core-Sérsic model is shown to coincide with the radius where it has a maximum in the second logarithmic derivative (Figure 9, right).
5. For the first time, the radius where the negative logarithmic slope of the light profile $\gamma' = 1/2$, considered to be a suitable estimator for the size of the core, is shown to be consistent with the core-Sérsic model break radius (Figure 11). It should, however, be noted that even galaxies without depleted cores will have a radius where γ' equals 1/2. Therefore, this measurement cannot be used to identify "true" depleted-core radii.
6. We have compared the core-Sérsic break radii with the Nuker break radii. In line with previous works, we found that the Nuker break radii are larger than the core-Sérsic break radii and also $R_{\gamma'=1/2}$: On average, the Nuker break radii are ∼2 times bigger than the core-Sérsic break radii. Furthermore, the surface brightnesses (μ_b) at the Nuker model's break radii are up to 2 mag arcsec^{-2} fainter than the surface brightness at the core-Sérsic model break radii.
7. We have updated various structural parameter relations after excluding galaxies that do not have "real" cores, and using core-Sérsic parameters. We have also used the bulge magnitude instead of the galaxy magnitude for the disk galaxies. We provide updated R_b–L, R_b–σ, R_b–μ_b, μ_b–L, and μ_b–σ relations in Section 7.1.
8. In contrast to Lauer et al. (2007a), we found consistency among three linear R_b–$M_{\rm BH}$ relationships (Section 7.2). While one of these is obtained directly from R_b and $M_{\rm BH}$ data (Equation (12)), the other two are constructed by combining the R_b–σ and $M_{\rm BH}$–σ relations and the R_b–L and $M_{\rm BH}$–L relations.
9. We detected additional nuclear light in 12 of the 39 sample galaxies. While our sample is rich in "core" galaxies (32/39), 5 of the 12 nucleated galaxies are Sérsic galaxies: one with nonthermal emission from an AGN and four with excess stellar light. Five of the seven nucleated "core" galaxies have AGN emission. These results are in good agreement with previous estimates (e.g., Rest et al. 2001; Côté et al. 2006).
10. Following Graham (2004), we derived a tentative central mass deficit for our "core" galaxies using Equation (A19) from Trujillo et al. (2004). These deficits are about 0.5 to 4 times the expected central SMBH hole mass.

This research was supported under the Australian Research Council's funding scheme (DP110103509 and FT110100263). This research has made use of the NASA/IPAC Extragalactic Database (NED) which is operated by the Jet Propulsion Laboratory, California Institute of Technology, under contract with the National Aeronautics and Space Administration.

APPENDIX A

In Figures 22–23 we show the fits to the major axis surface brightness profiles of the galaxies in Table 1.

APPENDIX B

B.1. Notes on Selected Individual Galaxies

NGC 584. This galaxy has a depleted core with an inner negative logarithmic slope $\gamma = 0.46$. Thus, it has $0.3 < \gamma < 0.5$ as opposed to the core ($\gamma < 0.3$) / power-law ($\gamma > 0.5$) dichotomy (see also Glass et al. 2011).

NGC 1374. This galaxy hosts an elongated inner disk (van der Marel & Franx 1993), which is well fit with a Sérsic model plus an inner exponential function for representing the disk.

NGC 3607. There is vivid evidence for the presence of an inner dust ring (Lauer et al. 2005).

NGC 3640. The galaxy is known for its morphological peculiarity including several sharp and diffuse features (e.g., shells, ripples), which probably signal an ongoing or recent merger (Michard & Prugniel 2004), which makes the underlying host galaxy light difficult to model since our model is not designed to accommodate such peculiarities. An ongoing or recent merger could be the reason for having an unusually small core for a galaxy of this luminosity.

NGC 3706. This galaxy exhibits an obvious inner stellar ring, shifting the peak of the surface brightness to $R \approx 0\farcs14$ from the photometric center (Lauer et al 2005). The light profile is better modeled with careful omission of the additional ring of starlight from $0\farcs11$ to $0\farcs4$ (see also Capetti & Balmaverde 2005).

NGC 4073. A cD galaxy with a possible history of cannibalism and having similar distinct features as NGC 3706. Lauer et al. (2005) identified an asymmetric central ring of stars noticeable on the brightness profile of the galaxy. Data points from $0\farcs1$ to $0\farcs4$ are excluded from the fit.

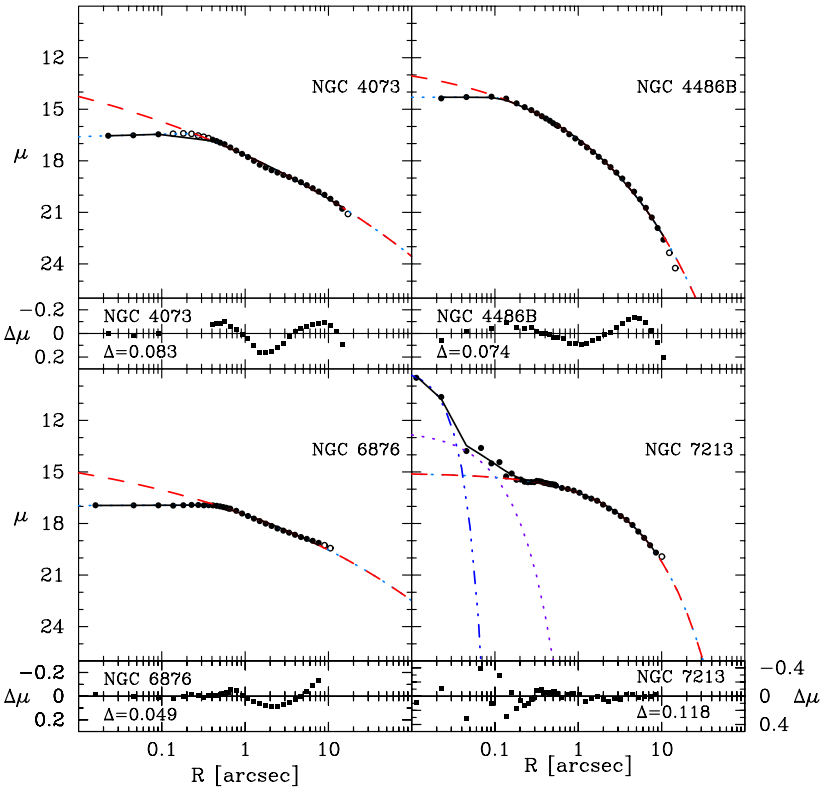

Figure 23. Similar to Figure 22, but for galaxies with various morphological peculiarities. See Appendix B text for further details.
(A color version of this figure is available in the online journal.)

NGC 4365. This object is a giant elliptical in the Virgo cluster with a kinematically distinct core (Forbes 1994) that has a slightly elongated inner nuclear excess (Carollo et al. 1997; Côté et al. 2006). The surface brightness profile is well fitted with the core-Sérsic model plus a Gaussian function for the inner nucleus.

NGC 4458. The isophotal contour analysis presented in Trujillo et al.'s. (2004) revealed a prominent nuclear disk, see also Morelli et al. (2004). Analysis of the brightness profile indicates the presence of an extended point source (Ferrarese et al. 2006) and an inner disk. A good match to the *HST*-observed profile is obtained fitting a Sérsic model plus an inner exponential ($n = 1$) disk component and a Gaussian ($n = 0.5$) for the point source.

NGC 4478. Like NGC 4458, there is evidence for the presence of a nuclear disk in this galaxy (e.g., Trujillo et al. 2004; Morelli et al. 2004). The only noticeable difference with the light profile of NGC 4458 is that this galaxy has a relatively elongated disk, and a compact point source (Carollo et al. 1997; Ferrarese et al. 2006).

NGC 4486B. Based on the deconvolved *HST*/WFPC2 *I*- and *V*-band images, Lauer et al. (1996) showed the existence of a double optical nucleus in this galaxy. However, the double nuclei are not obvious from most of the archival optical *HST* images, as noted by Ferrarese et al. (2006), and it may be an artifact of the deconvolution routine. Nonetheless, the plateau in the inner light profile is not due to a relative deficit of stars. Tidal truncation from the interaction with the close companion M87 is apparent from the fit to the surface brightness profile, particularly in the outer part of the profile ($R > 7'' \approx 0.7$ kpc).

NGC 4552. This galaxy hosts a compact point source, which is detectable in the optical image (Renzini et al. 1995; Carollo et al. 1997; Cappellari et al. 1999; Lauer et al. 2005).

NGC 5419. There seem to be two compact nuclear point sources, the brighter one at the photometric center, visible in the optical images (e.g., Capetti & Balmaverde 2005; Lauer et al. 2005). A "dip," in the region 0.″1–0.″2, is detected in the light profile of the galaxy. Thus, two data points from $0.''1 < R < 0.''2$ are excluded from the fit.

NGC 6876. The dominant elliptical in the Pavo group shows past or ongoing interaction with the large spiral NGC 6872 (Machacek et al. 2005). Furthermore, the archival *I*- and *V*-band images of this galaxy indicate the presence of a double optical nucleus (Figure 4), possibly the semi-digested nuclei of lesser galaxies or the ends of an inclined ring (Lauer et al. 2002). Like NGC 4486B, a core-Sérsic model can fit the surface brightness profile (see Figure 23). Although, as the nuclei appear only 0.″16, and equidistant, from the center, they may not explain the core's structure and break radius of 0.″45.

NGC 7213. This galaxy is the only spiral (Sa) in our sample. It hosts a bright Seyfert nucleus (Véron-Cetty & Véron 1988) and an inner disk. Hameed et al. (2001), see also Grosbøl et al. (2004), argue, based on the H I (neutral hydrogen) map, that this a highly disturbed system that may have experienced a past merger. In addition, using the broadband *HST* images, Deo et al. (2006) noted nuclear dust features in this galaxy.

REFERENCES

Allen, P. D., Driver, S. P., Graham, A. W., et al. 2006, MNRAS, 371, 2
Andredakis, Y. C., Peletier, R. F., & Balcells, M. 1995, MNRAS, 275, 874
Balcells, M., Graham, A. W., Domíngez-Palmero, L., & Peletier, R. F. 2003, ApJ, 582, L79
Balmaverde, B., & Capetti, A. 2006, A&A, 447, 97
Begelman, M. C., Blandford, R. D., & Rees, M. J. 1980, Nature, 287, 307
Bekki, K., & Graham, A. W. 2010, ApJ, 714, L313
Bell, E. F., Wolf, C., Meisenheimer, K., et al. 2004, ApJ, 608, 752
Bernardi, M., Alonso, M. V., daCosta, L. N., et al. 2002, AJ, 123, 2990

Binney, J., & Mamon, G. A. 1982, MNRAS, 200, 361
Biretta, J., et al. 2001, WFPC2 Instrument Handbook, Version 6.0 (Baltimore, MD: STScI)
Blakeslee, J. P., Lucey, J. R., Tonry, J. L., et al. 2002, MNRAS, 330, 443
Byun, Y.-I., Grillmair, C. J., Faber, S. M., et al. 1996, AJ, 111, 1889
Caon, N., Capaccioli, M., & D'Onofrio, M. 1993, MNRAS, 265, 1013
Capetti, A., & Balmaverde, B. 2005, A&A, 440, 73
Cappellari, M., Renzini, A., Greggio, L., et al. 1999, ApJ, 519, 117
Carollo, C. M., Franx, M., Illingworth, G. D., & Forbes, D. A. 1997, ApJ, 481, 710
Condon, J. J., Cotton, W. D., Greisen, E. W., et al. 1998, AJ, 115, 1693
Condon, J. J., Cotton, W. D., Greisen, E. W., et al. 2002, VizieR Online Data Catalog, 8065, 0
Côté, P., Ferrarese, L., Jordán, A., et al. 2007, ApJ, 671, 1456
Côté, P., Piatek, S., Ferrarese, L., et al. 2006, ApJS, 165, 57
Cox, T. J., Jonsson, P., Primack, J. R., & Somerville, R. S. 2006, MNRAS, 373, 1013
Crane, P., Stiavelli, M., King, I. R., et al. 1993, AJ, 106, 1371
Davies, R. L., Efstathiou, G., Fall, S. M., Illing- worth, G., & Schechter, P. L. 1983, ApJ, 266, 41
Deo, R. P., Crenshaw, D. M., & Kraemer, S. B. 2006, AJ, 132, 321
de Ruiter, H. R., Parma, P., Capetti, A., et al. 2005, A&A, 439, 487
de Vaucouleurs, G. 1948, Ann. Astrophys., 11, 247
de Vaucouleurs, G., de Vaucouleurs, A., Corwin, H. G., Jr., et al. 1991, Third Reference Catalogue of Bright Galaxies (Berlin: Springer)
Dhar, B. K., & Williams, L. L. R. 2010, MNRAS, 405, 340
Dhar, B. K., & Williams, L. L. R. 2011, arXiv:1112.3120
Diehl, S., & Statler, T. S. 2008, ApJ, 680, 897
Djorgovski, S., & Davis, M. 1987, ApJ, 313, 59
D'Onofrio, M., Capaccioli, M., & Caon, N. 1994, MNRAS, 271, 523
Faber, S. M., Tremaine, S., Ajhar, E. A., et al. 1997, AJ, 114, 1771
Feigelson, E. D., & Babu, G. J. 1992, ApJ, 397, 55
Ferrarese, L., Côté, P., Jordán, A., et al. 2006, ApJS, 164, 334
Ferrarese, L., & Merritt, D. 2000, ApJ, 539, L9
Ferrarese, L., van den Bosch, F. C., Ford, H. C., Jaffe, W., & O'Connell, R. W. 1994, AJ, 108, 1598
Ferrari, F., Dottori, H., Caon, N., Nobrega, A., & Pavani, D. B. 2004, MNRAS, 347, 824
Forbes, D. A. 1994, AJ, 107, 2017
Fukugita, M., Shimasaku, K., & Ichikawa, T. 1995, PASP, 107, 945
Gebhardt, K., Bender, R., Bower, G., et al. 2000, ApJ, 539, L13
Gebhardt, K., Lauer, T. R., Pinkney, J., et al. 2007, ApJ, 671, 1321
Gebhardt, K., Richstone, D., Ajhar, E. A., et al. 1996, AJ, 112, 105
Glass, L., Ferrarese, L., Côté, P., et al. 2011, ApJ, 726, 31
Goerdt, T., Moore, B., Read, J. I., & Stadel, J. 2010, ApJ, 725, 1707
Graham, A. W. 2004, ApJ, 613, L33
Graham, A. W. 2007, MNRAS, 379, 711
Graham, A. W. 2008a, ApJ, 680, 143
Graham, A. W. 2008b, PASA, 25, 167
Graham, A. W. 2012a, in Planets, Stars and Stellar Systems (Springer), in press (arXiv:1108.0997)
Graham, A. W. 2012b, ApJ, 746, 113
Graham, A. W., & Driver, S. P. 2005, PASA, 22, 118
Graham, A. W., Erwin, P., Trujillo, I., & Asensio Ramos, A. 2003, AJ, 125, 2951
Graham, A. W., & Guzmán, R. 2003, AJ, 125, 2936
Graham, A. W., Lauer, T. R., Colless, M. M., & Postman, M. 1996, ApJ, 465, 534
Graham, A. W., Onken, C. A., Athanassoula, E., & Combes, F. 2011, MNRAS, 412, 2211
Graham, A. W., & Worley, C. C. 2008, MNRAS, 388, 1708
Grillmair, C. J., Faber, S. M., Lauer, T. R., et al. 1994, AJ, 108, 102
Grosbøl, P., Patsis, P. A., & Pompei, E. 2004, A&A, 423, 849
Gualandris, A., & Merritt, D. 2012, ApJ, 744, 74
Gültekin, K., Richstone, D. O., Gebhardt, K., et al. 2009, ApJ, 695, 1577
Gültekin, K., Richstone, D. O., Gebhardt, K., et al. 2011, ApJ, 741, 38
Hameed, S., Blank, D. L., Young, L. M., & Devereux, N. 2001, ApJ, 546, L97
Hernquist, L. 1990, ApJ, 356, 359
Hernquist, L. 1993, ApJ, 409, 548
Hopkins, P. F., Cox, T. J., Ditta, S. N., et al. 2009, ApJS, 181, 135
Hopkins, P. F., & Hernquist, L. 2010, MNRAS, 407, 447
Jaffe, W., Ford, H. C., O'Connell, R. W., van den Bosch, F. C., & Ferrarese, L. 1994, AJ, 108, 1567
Kandrup, H. E., Sideris, I. V., Terzić, B., & Bohn, C. L. 2003, ApJ, 597, 111
Khochfar, S., & Burkert, A. 2003, ApJ, 597, 117
King, I. R. 1978, ApJ, 222, 1
King, I. R., & Minkowski, R. 1966, ApJ, 143, 1002
King, I. R., & Minkowski, R. 1972, in IAU Symp. 44, External Galaxies and Quasi-Stellar Objects, ed. D. S. Evans, D. Wills, & B. J. Wills (Dordrecht: Reidel), 87
Kormendy, J. 1999, in ASP Conf. Ser. 182, Galaxy Dynamics—A Rutgers Symposium, ed. D. R. Merritt, M. Valluri, & J. A. Sellwood (San Francisco, CA: ASP), 124
Kormendy, J., & Bender, R. 2009, ApJ, 691, L142
Kormendy, J., Dressler, A., Byun, Y. I., et al. 1994, in ESO/OHP Workshop on Dwarf Galaxies, ed. G. Meylan & P. Prugniel (Garching: ESO), 147
Kormendy, J., Fisher, D. B., Cornell, M. E., & Bender, R. 2009, ApJS, 182, 216
Kulkarni, G., & Loeb, A. 2012, MNRAS, 422, 1306
Laine, S., van der Marel, R. P., Lauer, T. R., et al. 2003, AJ, 125, 478
Lauer, T. R., Ajhar, E. A., Byun, Y.-I., et al. 1995, AJ, 110, 2622
Lauer, T. R., Faber, S. M., Gebhardt, K., et al. 2005, AJ, 129, 2138
Lauer, T. R., Faber, S. M., Richstone, D., et al. 2007a, ApJ, 662, 808
Lauer, T. R., Gebhardt, K., Faber, S. M., et al. 2007b, ApJ, 664, 226
Lauer, T. R., Gebhardt, K., Richstone, D., et al. 2002, AJ, 124, 1975
Lauer, T. R., Tremaine, S., Ajhar, E. A., et al. 1996, ApJ, 471, L79
Laurikainen, E., Salo, H., Buta, R., Knapen, J. H., & Comerón, S. 2010, MNRAS, 405, 1089
Lyubenova, M., Kuntschner, H., & Silva, D. R. 2008, A&A, 485, 425
Machacek, M., Nulsen, P. E. J., Stirbat, L., Jones, C., & Forman, W. R. 2005, ApJ, 630, 280
Makino, J., & Ebisuzaki, T. 1996, ApJ, 465, 527
Marconi, A., & Hunt, L. K. 2003, ApJ, 589, L21
Martizzi, D., Teyssier, R., & Moore, B. 2012, MNRAS, 420, 2859
Merritt, D. 2006, ApJ, 648, 976
Merritt, D., & Milosavljević, M. 2005, Living Rev. Relativ., 8, 8
Michard, R., & Prugniel, P. 2004, A&A, 423, 833
Milosavljević, M., & Merritt, D. 2001, ApJ, 563, 34
Morelli, L., Halliday, C., Corsini, E. M., et al. 2004, MNRAS, 354, 753
Naab, T., Jesseit, R., & Burkert, A. 2006, MNRAS, 372, 839
Naab, T., & Ostriker, J. P. 2009, ApJ, 690, 1452
Nakano, T., & Makino, J. 1999, ApJ, 510, 155
Nieto, J.-L., Bender, R., & Surma, P. 1991, A&A, 244, L37
Nieto, J.-P., & Bender, R. 1989, A&A, 215, 266
Paturel, G., Petit, C., Prugniel, P., et al. 2003, A&A, 412, 45
Pellegrini, S. 2010, ApJ, 717, 640
Ravindranath, S., Ho, L. C., Peng, C. Y., Filippenko, A. V., & Sargent, W. L. W. 2001, AJ, 122, 653
Renzini, A., Greggio, L., di Serego Alighieri, S., et al. 1995, Nature, 378, 39
Rest, A., van den Bosch, F. C., Jaffe, W., et al. 2001, AJ, 121, 2431
Richings, A. J., Uttley, P., & Kröding, E. 2011, MNRAS, 415, 2158
Sérsic, J. L. 1963, Bol. Asociación Argentina Astron., 6, 41
Sérsic, J. L. 1968, Atlas de Galaxias Australes (Cordoba: Observatorio Astronomico)
Soldatenkov, D. A., Vikhlinin, A. A., & Pavlinsky, M. N. 2003, Astron. Lett., 29, 298
Somerville, R. S., & Primack, J. R. 1999, MNRAS, 310, 1087
Soria, R., Graham, A. W., Fabbiano, G., et al. 2006, ApJ, 640, 143
Tonry, J. L., Dressler, A., Blakeslee, J., et al. 2001, ApJ, 546, 681
Toomre, A., & Toomre, J. 1972, ApJ, 178, 623
Trujillo, I., Erwin, P., Asensio Ramos, A., & Graham, A. W. 2004, AJ, 127, 1917
van den Bosch, F. C., Ferrarese, L., Jaffe, W., Ford, H. C., & O'Connell, R. W. 1994, AJ, 108, 1579
van der Marel, R. P., & Franx, M. 1993, ApJ, 407, 525
Véron-Cetty, M.-P., & Véron, P. 1988, A&A, 204, 28
White, R. L., & Becker, R. H. 1992, ApJS, 79, 331
Worthey, G. 1994, ApJS, 95, 107
Xu, C. K., Zhao, Y., Scoville, N., et al. 2012, ApJ, 747, 85
Young, C. K., & Currie, M. J. 1994, MNRAS, 268, L11
Younes, G., Porquet, D., Sabra, B., et al. 2010, A&A, 517, 33
Young, P. J., Westphal, J. A., Kristian, J., Wilson, C. P., & Landauer, F. P. 1978, ApJ, 221, 721